Realia et naturalia

DISSERTATIONES
PHYSICAE
UNIVERSITATIS
TARTUENSIS
95

TAAVI VAIKJÄRV

Consideration of non-adiabaticity of the Pseudo-Jahn-Teller effect: contribution of phonons

TARTU ÜLIKOOL
1632
UNIVERSITAS TARTUENSIS

DISSERTATIONES PHYSICAE UNIVERSITATIS TARTUENSIS
95

DISSERTATIONES PHYSICAE UNIVERSITATIS TARTUENSIS
95

TAAVI VAIKJÄRV

Consideration of non-adiabaticity of the Pseudo-Jahn-Teller effect: contribution of phonons

UNIVERSITY OF TARTU
PRESS
1632

This study was carried out at the University of Tartu.

The dissertation was admitted on 11.11.2014 in partial fulfilment of the requirements for the degree of Doctor of Philosophy in Physics, and was allowed for defence by the Council of the Institute of Physics, University of Tartu.

Supervisors: DSc Vladimir Hizhnyakov, University of Tartu, Estonia

Opponents: Prof. Ernst Sigmund, Technical University of Brandenburg, Cottbus, Germany

PhD Mihhail Klopov, Tallinn University of Technology, Tallinn, Estonia

Defence: January 16, 2015, at the University of Tartu

The research presented in this thesis is supported by the Estonian Science Foundation projects no. ETF7741 and IUT2-27.

ISSN 1406-0647
ISBN 978-9949-32-737-9 (print)
ISBN 978-9949-32-738-6 (pdf)

University of Tartu Press
www.tyk.ee

TABLE OF CONTENTS

LIST OF ORIGINAL PUBLICATIONS

This thesis is based on the following publications (full texts included at the end of the thesis), which are referred to in the text by their Roman numerals. The papers are reprinted with the kind permission from the publishers.

I V. Hizhnyakov, K. Pae, T. Vaikjärv Vibronic Transitions to a State with Jahn-Teller Effect: Contribution of Phonons, in Vibronic Interactions and the Jahn-Teller Effect: Theory and Applications, M.Atanasov et al. (Eds.), (2012), 179–191, Springer.

II I. Tehver, G. Benedek, V. Boltrushko, V. Hizhnyakov, T. Vaikjärv Raman Scattering for Weakened Bonds in the Intermediate States of Impurity Centres, in Vibronic Interactions and the Jahn-Teller Effect: Theory and Applications, M.Atanasov et al. (Eds.), (2012), 163–177, Springer.

III V. Hizhnyakov, V. Boltrushko, K. Pae, T. Vaikjarv, Zero-phonon lines: Novel manifestations of vibronic interactions in impurity centres of solids. Optika i Spektroskopiya, **111(3)**, (2011), 377–385.

IV V. Hizhnyakov, K. Pae, T. Vaikjärv. Optical Jahn-Teller effect in the case of local modes and phonons. Chemical Physics Letters, **525–526**, (2012), 64–68.

V T. Vaikjärv, V. Hizhnyakov, Time-dependent pseudo Jahn-Teller effect: Phonon-mediated long-time nonadiabatic relaxation. Journal of Chemical Physics, **140 (6)**, (2014), 064105.

Author's contribution

The articles were elaborated in collaboration with all the researchers involved. The author of this thesis was responsible for the development of the numerical methods for the calculations concerning the pseudo-Jahn-Teller effect and provided the figures and the interpretation of the results based on the results of the calculations. The task of verifying the derivation of the theoretical model was also necessary in the process. In the last article he also had the leading role of writing the main body of the text.

ABBREVIATIONS

JT	Jahn-Teller
JTE	Jahn-Teller effect
PJTE	pseudo Jahn-Teller effect
PEC	Potential energy curve
REP	Raman excitation profile

1. INTRODUCTION

1.1 Overview of the Jahn-Teller effect

In 1937 Hermann Jahn and Edward Teller published a paper [1] where they analyzed all symmetry groups corresponding to degenerate electronic states in polyatomic molecules. They found that all groups except the ones corresponding to linear molecules contained a nontotally symmetric representation. This meant that there existed a direction, where the movement of nuclei removes the degeneracy, thus reducing the energy of the system. They finally concluded that „*stability and degeneracy are not possible simultaneously unless the molecule is a linear one*". This became known as the Jahn-Teller (JT) theorem and the phenomenon of molecule distortions explained by this theorem as JT effect (JTE). A similar effect was also discussed to occur in linear molecules, called the Renner-Teller effect [2], and in the molecules with quasi-degenerate electronic states, called pseudo JTE (PJTE). The PJTE was considered by Öpik and Pryce in 1957 [3] as a small perturbation from the original JTE. The PJTE, however, is in itself a valuable tool in understanding molecular dynamics. "*The PJTE is the only source of instability and distortions of high-symmetry configurations of polyatomic systems in non-degenerate states, and it contributes essentially to the instability of degenerate states*" [4]. The two effects, however, are closely related, as they are a result of the same nuclear-electron coupling effect. For the JTE to occur a degenerate electronic state coupled by vibrations is required. In the PJTE case no degeneracy is needed. The only requirement is the existence of vibronically coupled electronic states. For the effect to be significant the states should be close in energy, as the coupling is reduced inversely to the separation in energy. However, electronic states as far as 10 eV [5] or 14 eV [4] apart can be coupled by the PJTE. It is worth noting that the two effects are not necessarily coexistent or simultaneously exclusive. In fact their strengths, if present in a system, are in no way correlated. Bersuker has suggested [6] that the whole JT theorem should be reformulated to include all the effects mentioned: „*The necessary and sufficient condition of instability of the high-symmetry configuration of any polyatomic system is the presence of two or more electronic states that are either degenerate in this configuration, or non-degenerate but sufficiently strongly interacting under nuclear displacements in the direction of instability, the twofold spin degeneracy being an exception.*"

Jahn and Teller started off a field of research into coupling effects between electronic and vibrational (vibronic) motions. The implications of this effect reach far beyond the simple understanding of molecular distortions. The most profound impact of the JTE has probably been on quantum chemistry, as the JT distortions influence the molecular dynamics. This has allowed to gain an insight into complex molecular processes, for example in photochemistry. High-temperature superconductivity is another example of a field influenced by the JTE. This time the electron-phonon mechanism for the formulation of Cooper

pairs can also be viewed as a JTE. The JTE also proves its value in describing the influence of the surrounding crystal on single molecular magnets and in spectroscopy of transition metal complexes. For a more detailed description of the field, its background, formalism and its applications, the books for example by Englman [7], Bersuker [8], Köppel et al. [9], should be consulted.

1.2 Purpose of the thesis

One of the most important goals for describing any quantum mechanical system is to write down its Hamiltonian and to find its eigenvalues. The adiabatic approximation is widely used [10] in discussing JTE and PJTE problems. It uses the inequality of nuclear and electron masses to solve the Hamiltonian of the system in two parts. Firstly, the electronic part is solved with the nuclear configuration taken as a parameter of the equation. In other words, the nuclear motion is taken to be much slower than the electronic motion. Secondly, the nuclear motion is found in the mean field of electrons. The adiabatic approximation works well if the electronic levels are well separated as compared to the quanta of vibrations. However, if important electronic levels are situated closely or if they are degenerate, the approximation fails. The aim of this thesis is to avoid the adiabatic approximation and to solve the problem in a way that non-adiabaticity be considered as well.

This thesis is only concerned with the PJTE and only from a theoretical point of view. For simplicity reasons further consideration is restricted to one of the simplest PJTE systems, namely the case of a dimer. Fulton and Gouterman [11] have shown that the dimeric Hamiltonian can be transformed in the same manner as a molecular one. The dimer is a better test system than a molecule, since it consists of two structurally similar subunits in interaction with each other. This guarantees that there exist two energy levels that have a similar potential energy curve (PEC) and that are similar in energy. The interaction between the subunits is necessary for a vibrational mode to mix the energy levels and for the PJTE to appear. The idea in this thesis is to also take into account all the other modes up to the full phonon continuum. This could represent a dimer embedded in a crystal medium. The interaction between the subunits of the dimer means that the interaction of one bath mode has been enhanced. In other words, there exist two energy levels mixed by an interaction with one vibrational mode and influenced by a continuum of weaker modes.

The energy diagram pictured in Figure 1 gives an overview of the processes involved.

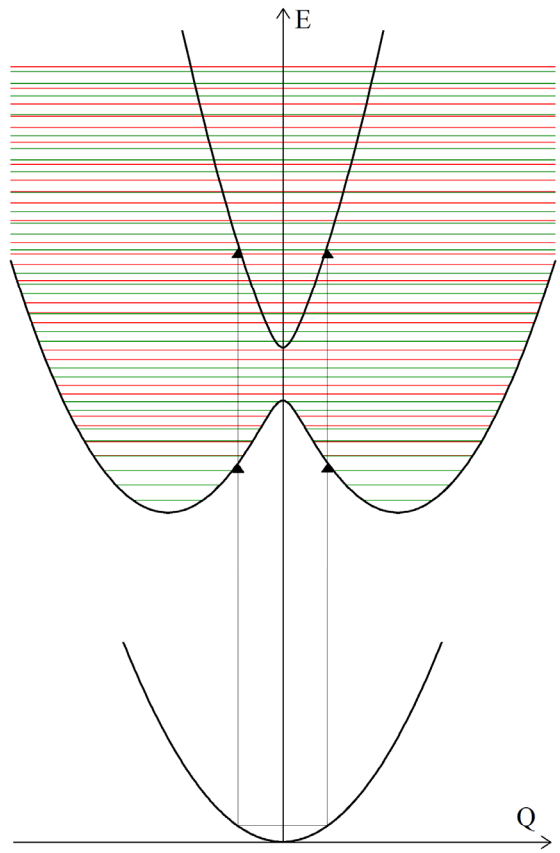

Figure 1: The qualitative shape of the potential energy curves for a transition from a non-degenerate to a vibronically coupled quasi-degenerate excited state. The red and green lines represent the vibronic levels associated with the upper and lower curve, respectively.

The effect of non-totally symmetric vibrations on the electronic transition from a non-degenerated to the two-fold quasi-degenerated electronic state of an impurity centre in solids is of interest. The considerations are restricted to the zero temperature case, as the theory is more transparent and the results can be highlighted better. An electron in an initial electronic ground state is excited to one of the two electronic states that are in interaction with each other. The vibrational mode is represented by a configurational coordinate Q (same idea was used in [12]). This coordinate is considered to be a linear combination of the normal coordinate of the local mode and normal coordinates of phonons. The local mode describes mainly the dimer and the phonon coordinates describe the interaction with the surrounding medium (bulk crystal). The contribution of bulk phonon coordinates to Q is supposed to be small compared to the contribution of the local mode, but not negligible. The theory holds also in the

case when the main motion of the dimer is described by a long-living pseudolocal mode [13]. The vibrationally coupled electronic energy levels form two PECs in the Q-space: the upper energy curve steeper than the initial energy level (the force constant has stiffened due to interaction) and the lower energy curve with two minima and an unstable maximum (flatter curve with reduced force constants). The vibronic energy levels arising from the interaction with the main mode are in close proximity and get mixed due to the phonons in the medium. This can be seen in the optical spectra, as is explained in section three. This mixing is also responsible for the non-radiative relaxation of the electron to the lower vibronic states, as is explained in section four. The non-radiative emission of the dimer's energy is possible by creating propagating phonons in the bulk.

The thesis is divided into three larger parts. The second section gives a theoretical framework of a novel way of considering the vibronic coupling. A strong interaction with one main mode of phonons that couples the two electronic states is required, however, the weak interaction with the whole phonon continuum is also taken into account. The main idea is to rewrite the Hamiltonian so that the vibronic interaction is transferred into the main mode in the ground electronic state. The eigenvalue problem for the ground state can easily be solved numerically. The influence of phonons on the main mode is taken into account by using the second cumulant expansion. In the third section, the obtained results are applied in the calculations of the optical spectra of dimers. The absorption spectrum and first- and second-order Raman excitation profiles (REP) are found. As the theory incorporates several hundreds of modes of the bulk and is applicable in a weak interaction limit, some novel results are presented. In the fourth section the aforementioned approach is used for calculating the lifetimes of the vibronic excited states that are influenced by bulk phonons. From this information the time dependence of the density matrix can be calculated. The density matrix can be used to find the time evolution of any observable quantity in the excited system, for example the wave function of the configurational coordinate.

2. THEORY OF VIBRONIC COUPLING

We will start with writing down the Hamiltonian of the system.

$$H_g = \frac{1}{2}\sum_j \left(-\frac{\partial^2}{\partial x_j^2} + \omega_j^2 x_j^2 \right) \tag{1}$$

is the vibrational Hamiltonian of the initial electronic state in the harmonic approximation (all the powers of displacement larger than 2 are neglected), x_j are the corresponding normal coordinates, ω_j are their frequencies (in the units where $\hbar$=1).

$$H_e = H_g \cdot I + V \tag{2}$$

is the vibronic Hamiltonian of the excited (quasi-degenarate) electronic state, I is a 2x2 unit matrix and V is the vibronic coupling matrix that mixes the two states. The vibronic coupling is taken in the linear approximation [14]:

$$V = \begin{pmatrix} \varepsilon & kQ \\ kQ & -\varepsilon \end{pmatrix}, \tag{3}$$

where Q is the odd configurational coordinate of the dimer in the Fulton and Gouterman terminology, 2ε is the energy splitting between the quasi-degenerate states. The constant k shows the strength of the coupling between the quasi-degenerate states and can be calculated as the overlap of the electronic wave functions with respect to nuclear displacements. We are considering the case where the coordinate Q is the linear combination of a number of normal coordinates x_j, but the main contribution to Q is given by one normal coordinate x_0. In this case Q can be presented in the form

$$Q = \left(1+\lambda^2\right)^{-1/2} \left(x_0 + \lambda \sum_{j\geq 1} e_{1j} x_j \right), \tag{4}$$

where λ is a small dimensionless parameter, e_{1j} are the normalized polarization vectors showing the contribution of the j-th phonon mode into the amplitude and direction along which the atom 1 oscillates. The number of contributing phonons is considered to be arbitrary.

The most interesting effects described by the model of the dimer are related with the case corresponding to a strong interaction with the main mode and to a comparable electronic interaction. No analytical solution of the problem is possible in this case, even if $\lambda = 0$ (no phonons are involved in the vibronic

interaction). However, in the latter case the eigenstates and eigenvalues (energies) of the vibronic Hamiltonian in Eq. (2) can be successfully found numerically [15]. One can expect that this numerical solution could be used as the zero'th approximation also in the case of phonons, supposing that their contribution to vibronic coupling is reasonably small. To this end one would need to use this solution as a basis for the consideration of the effect caused by the phonon vibronic Hamiltonian:

$$V_{Ph} = \frac{k\lambda}{\sqrt{1+\lambda^2}} \begin{pmatrix} 0 & \sum_j e_j x_j \\ \sum_j e_j x_j & 0 \end{pmatrix}. \tag{5}$$

Unfortunately, it is a rather difficult task to rewrite V_{Ph} in the basis dioganalizing H_e, which is not explicitly solved until today.

However, the problem can be solved differently: one can replace the linear vibronic coupling V_{Ph} by the quadratic coupling of the main PJTE active mode x_0 with phonons. The effect of the latter Hamiltonian can be considered straightforwardly, while all the required matrix elements of x_0 in the numerically found basis diagonalizing H_e are known.

2.1 Transformation of vibronic interaction with phonons

The required transformation of V_{Ph} to the quadratic phonon Hamiltonian was first done in [I] and more generally in [IV] (for full derivation see Appendix A.1):

$$H_g \approx H_0 + H_{ph} + H', \tag{6}$$

where $H_0 = \omega_0 a_0^+ a_0$ and $H_{ph} = \sum_{j\geq 1} \omega_j a_j^+ a_j$ are the Hamiltonians of the main mode and phonons, respectively,

$$H' = \lambda \sum_{j\geq 1} \upsilon_j \left(a_0^+ + a_0\right)\left(a_j + a_j^+\right) \tag{7}$$

is the interaction of the main mode with phonons, a^+ and a are the creation and destruction operators,

$$\upsilon_j = e_{1j}\left(\omega_0^2 - \omega_j^2\right)\Big/ 2\sqrt{\omega_0 \omega_j}\,. \tag{8}$$

In the notation of the ladder operators the vibronic interaction gets the following form:

$$V = \begin{pmatrix} G & \sqrt{D}\left(a_0 + a_0^+\right) \\ \sqrt{D}\left(a_0 + a_0^+\right) & -G \end{pmatrix}, \tag{9}$$

where $D = k^2/2\omega_0$ is the vibronic interaction parameter. The units of ω_0 for the energy are used: $G = \varepsilon/\omega_0$. Consequently, as a result of the transformation, the linear vibronic interaction with non-totally symmetric phonons is replaced by the quadratic interaction H' of the main (JT-active) mode with phonons.

2.2 Vibronic basis

The eigenstates $\left|\nu^{\pm}\right\rangle$ of the vibronic Hamiltonian $H_0 \cdot I + V$ will be used as the basis for the further treatment. The eigenstates satisfy the equation

$$(H_0 \cdot I + V)\begin{pmatrix} \left|\nu^+\right\rangle \\ \left|\nu^-\right\rangle \end{pmatrix} = E_\nu \begin{pmatrix} \left|\nu^+\right\rangle \\ \left|\nu^-\right\rangle \end{pmatrix}. \tag{10}$$

If one were to expand the eigenstates $\left|\nu^{\pm}\right\rangle$ over the eigenstates $\left|n\right\rangle$ of the Hamiltonian H_g:

$$\left|\nu^{\pm}\right\rangle = \sum_n C_{n\nu}^{\pm} \left|n\right\rangle, \tag{11}$$

and after some manipulation (see Appendix A.2) Eq. (10) obtains a three-diagonal form

$$\begin{pmatrix} G & \sqrt{D} & 0 & 0 & \ldots \\ \sqrt{D} & 1-G & \sqrt{2D} & 0 & \ldots \\ 0 & \sqrt{2D} & 2+G & \sqrt{3D} & \ldots \\ 0 & 0 & \sqrt{3D} & 3-G & \ldots \\ \ldots & \ldots & \ldots & \ldots & \ldots \end{pmatrix} \begin{pmatrix} C_{0\nu}^+ \\ C_{1\nu}^- \\ C_{2\nu}^+ \\ C_{3\nu}^- \\ \ldots \end{pmatrix} = \nu \begin{pmatrix} C_{0\nu}^+ \\ C_{1\nu}^- \\ C_{2\nu}^+ \\ C_{3\nu}^- \\ \ldots \end{pmatrix},$$

$$\begin{pmatrix} -G & \sqrt{D} & 0 & 0 & \ldots \\ \sqrt{D} & 1+G & \sqrt{2D} & 0 & \ldots \\ 0 & \sqrt{2D} & 2-G & \sqrt{3D} & \ldots \\ 0 & 0 & \sqrt{3D} & 3+G & \ldots \\ \ldots & \ldots & \ldots & \ldots & \ldots \end{pmatrix} \begin{pmatrix} C_{0\nu}^- \\ C_{1\nu}^+ \\ C_{2\nu}^- \\ C_{3\nu}^+ \\ \ldots \end{pmatrix} = \nu \begin{pmatrix} C_{0\nu}^- \\ C_{1\nu}^+ \\ C_{2\nu}^- \\ C_{3\nu}^+ \\ \ldots \end{pmatrix}. \tag{12}$$

These equations can be solved by standard methods, supposing that one can restrict himself with a finite number of the states of the pseudolocal mode.

2.3 Contribution of phonons

In order to take into account the phonon effects we rewrite the Hamiltonian $H_g + V \approx H_0 + H_{ph} + H' + V = H_2 + H'$ and then use the Dyson equation [16] for the evolution operator $\mathrm{e}^{it(H_g+V)}$. An average of the evolution operator over zero-point states would give a Fourier transform of the absorption (discussed later). The case of strong vibronic coupling with the main mode and weak coupling with phonons is of interest. If the phonon coupling is sufficiently small, then one can take the interaction H' into account approximately by using the cumulant expansion. In this approximation we get (for details see Appendix A.3)

$$\left\langle 0\left|\mathrm{e}^{it(H_g+V)}\right|0\right\rangle \approx \sum_{\nu} |\, C^{\pm}_{0\nu}\,|^2 \exp\left[iE^{\pm}_{\nu}t + g^{\pm}_{\nu}(t)\right]. \qquad (13)$$

$$g^{\pm}_{\nu}(t) = -\int_0^t d\tau \int_0^{\tau} d\tau' \left\langle \nu_{\pm}\left|\left\langle 0_{ph}\left|H'(\tau)H'(\tau')\right|0_{ph}\right\rangle\right|\nu_{\pm}\right\rangle \qquad (14)$$

is the cumulant generating function up to the second-order cumulants. This function can be calculated by using the results from solving Eqs. (12)

$$g^{\pm}_{\nu}(t) = \lambda^2 \sum_j \upsilon_j^2 \sum_{\nu'} \left|S^{\pm}_{\nu\nu'}\right|^2 \left(\frac{-it}{E^{\pm}_{\nu} - E^{\mp}_{\nu'} - \omega_j} + \frac{e^{i\left(E^{\pm}_{\nu} - E^{\mp}_{\nu'} - \omega_j\right)t} - 1}{\left(E^{\pm}_{\nu} - E^{\mp}_{\nu'} - \omega_j\right)^2} \right), \qquad (15)$$

$$S^{+}_{\nu\nu'} = s^{+}_{\nu\nu'} + s^{-}_{\nu\nu'}; \quad s^{\pm}_{\nu\nu'} = \sum_n C^{\pm}_{2n+1,\nu} \left(\sqrt{2n+1}\, C^{\mp}_{2n,\nu'} + \sqrt{2n+2}\, C^{\mp}_{2n+2,\nu'} \right). \qquad (16)$$

2.4 Change of frequency

Let us consider the transition from a ground state to an excited state with different frequencies of the harmonic oscillators of the corresponding Hamiltonians H_g and H_e. This will change the vibronic states. This was first done by Pae [17] by making use of the results on generating functions from Kubo ja Toyozawa [18]. An expansion of the ground initial state through the eigenstates of the excited state would be

$$\left|0\right\rangle_g = \sum_n s_{2n} \left|2n\right\rangle_e, \qquad (17)$$

the coefficients s_{2n} being (for derivation see Appendix A.4)

$$s_{2n} = \sqrt{\frac{2(2n-1)!!\sqrt{\omega_i \omega_f}}{2^n n!(\omega_i + \omega_f)}} \left(\frac{\omega_i - \omega_f}{\omega_i + \omega_f} \right)^n . \qquad (18)$$

The frequency change is described by the quadratic term in the vibrational Hamiltonian with respect to the vibrational coordinate. Therefore, only even states give a contribution to new even vibrational states.

2.5 Model of phonons

In the following discussion the Debye-Van Hove model of phonons is used. This model accurately describes the acoustic phonons in the region of high and low frequencies. In Eq. (15) the υ_j^2 function is taken as (see Appendix A.5)

$$\upsilon^2(\omega) = e^2(\omega) \frac{\left(\omega_0^2 - \omega^2\right)^2}{4\omega_0 \omega} = \frac{8\omega^3}{\pi \omega_0 \omega_M^6} \left(\omega_0^2 - \omega^2\right)^2 \sqrt{\omega_M^2 - \omega^2} , \qquad (19)$$

where ω_M is the maximum frequency of phonons. The phonon distribution can be seen in Figure 2.

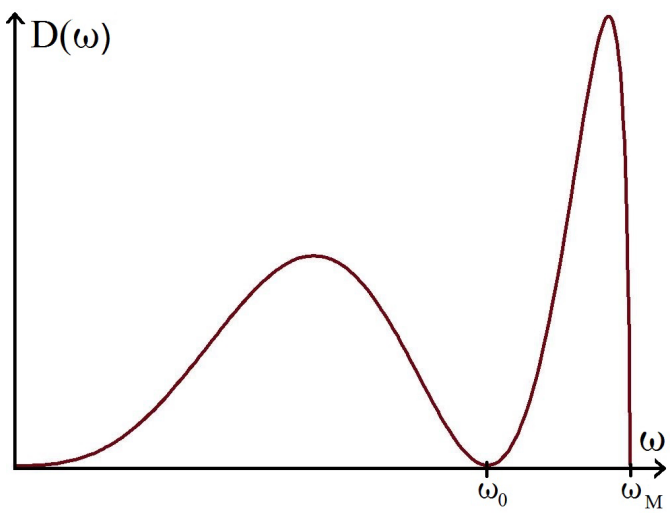

Figure 2. Transformed phonon density of states, where the main mode has been excluded

The main implication from the phonon distribution for the further treatment is that in Eq. (15) the summation over ν' can be reduced to summation over $\nu' = \nu \pm 1$. The idea is that the energy of phonons is not sufficient to be responsible for larger transitions. The energy difference between the vibronic lines ν and $\nu + 1$ is in the order of ω_0. The value of maximum phonon frequency has been taken $\omega_M = 1.3\omega_0$, being smaller than the difference between the second neighbour energy levels.

3. OPTICAL SPECTRA

One of the simplest methods for obtaining experimental data about PJTE systems is the optical probing. The current theory can be applied to predict the optical spectra of these systems. Here absorption spectra as well as first- and second-order Raman excitation profiles (REPs) are considered. REP - the relationship between excitation frequency and integral Raman scattering energy - is of special interest. It gives complementary information to absorption, since the vibronic coupling effects can be seen easily. This is very important in multimode systems, since different modes can be distinguished. Also, many similar features in absorption spectra can be of different origin. However, their Raman spectra are different and thus they can be distinguished. Raman spectroscopy has one more advantage over absorption. The resonant Raman spectroscopy methods could yield spectra with very fine details even from the samples with very low concentration. Thus, we will proceed with the emphasis on finding REPs.

It was first suggested by Lax [19] that absorption is easily described in the time domain. The spectrum is determined by

$$F_i(t) = \left\langle i \left| \mu_\alpha e^{itH_e} \mu_\alpha e^{-itH_g} \right| i \right\rangle, \tag{20}$$

where F is the Fourier transform of the absorption spectrum, μ_α are the electric dipole moment operators. $\alpha = x, y$ denote the two axes of polarization . $|i\rangle$ is the initial vibrational state in the ground electronic state. Hizhnyakov and Tehver [20] have analogously expanded this idea to the case of resonant Raman scattering from an initial ground state to a final ground state $|f\rangle$.

$$A_{\alpha\beta,if}(t) = \Theta(t) \left\langle f \left| \mu_\beta e^{itH_e} \mu_\alpha e^{-itH_g} \right| i \right\rangle, \tag{21}$$

where $A_{\alpha\beta,if}$ is the Fourier transform of the resonance Raman scattering amplitudes. $\Theta(t)$ is the Heaviside step function that takes into account the causality in the equation (scattering follows excitation). If we consider the zero temperature, then the system is initially in the ground electronic and vibrational state $|i\rangle = |0\rangle|0\rangle$. The final state is then $|f\rangle = |k\rangle|0\rangle$, where $k = 0$ in the case of absorption and $k = 1, 2$ in the first- and second-order Raman scattering, respectively. In the proposed model non-totally symmetric vibrations are under consideration. This means that the phonons involved will change the polarization of the system. Since first- order Raman scattering is a one-phonon process and second-order Raman scattering is a two- phonon process, it follows from symmetry considerations that $A_{\alpha\beta,0f}$ is non-zero for all even orders of f when $\alpha = \beta$. Likewise, the odd orders of f are only non-zero if $\alpha \neq \beta$. This reduces the first-order Raman scattering into $A_1 \equiv A_{xy,01}$ and the second-order one into $A_2 \equiv A_{xx,02}$.

$$A_k(t) = \Theta(t)\langle k|\langle 0|\mu_x e^{itH_e}\mu_x e^{-itH_g}|0\rangle|0\rangle, \qquad (22)$$

Here the results of Eq. (13) can be used, the exception being that the state $|k\rangle$ will be expanded as $|k\rangle = \sum_\nu C_{k\nu}^{\pm}|\nu^{\pm}\rangle$. Also, the relations $\langle g|\mu_x|+\rangle_e = \langle g|\mu_x|-\rangle_e = M$ have to be taken into account, where M is a constant. This results in Eq. (22) becoming

$$A_k(t) \approx \Theta(t)M^2\sum_\nu C_{k\nu}C_{0\nu}\exp\left[iE_\nu t + g_\nu(t)\right]. \qquad (23)$$

The Fourier transform of the absorption spectrum is

$$F(t) \approx \sum_\nu |C_{0\nu}^{+}|^2 \exp\left[iE_\nu t + g_\nu(t)\right]. \qquad (24)$$

These equations can be interpreted in the following way. The Fourier transform of the $\exp(iE_\nu t)$ term to the frequency domain results in E_ν determining the frequencies of the vibronic lines. The constants $C_{k\nu}C_{0\nu}$ determine the relative intensities of these narrow lines (analogous results were obtained in [21]). It follows from Eq. (23) and Eq. (24) that the effects of phonons are described by the factors $\exp(g_\nu(t))$. The imaginary part of the function $g_\nu(t)$ gives a (small) correction to the position of the vibronic line. The real part changes the line shape. Every vibronic line is replaced by a phonon-assisted band whose shape is determined by the Fourier transform of $\exp(g_\nu(t))$.

3.1 Expected strength of vibronic effects

Before proceeding with the calculations of the spectra it would be useful to analyze in more detail the strength of phonon effects, as was also discussed in [IV]. The value of the function $g_\nu(t)$ determines the interaction of phonons with each vibronic level. For example, this value shows the lifetime of each vibronic line and the strength of phonon wings in the spectra. It is interesting to have some idea about the relative magnitude of the influences on each vibronic line. The value of the function $g_\nu(t)$ can vary greatly, as this depends reciprocally on the energy difference between vibronic levels (Eq. (15)). In Figure 3 (see also Figure 1) the energy difference between the nearest and second nearest vibronic energy levels is plotted.

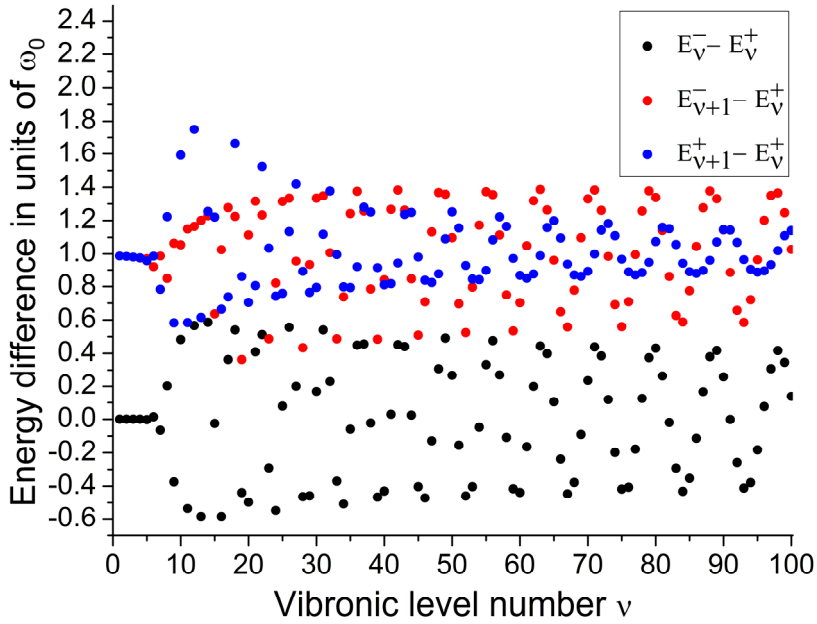

Figure 3. Energy difference between vibronic lines: a) different PEC and the same vibronic line number (black), b) different PEC and next neighbour vibronic line number (red) and c) the same PEC and next neighbour vibronic line number (blue)

There is a periodic pattern of spacing between the vibronic levels corresponding to different PEC. This leads to great variations in energy differences among vibronic lines, as can be seen from Figure 3. For a continuous spectrum of phonons there are phonons that make practically every vibronic transition possible. The maximum phonon frequency of $\omega_M = 1.3\omega_0$ is sufficient for the nearest and next nearest vibronic energy level transitions. The transitions between the energy levels of the same PEC are not possible by non-totally symmetric phonons, however, the energy difference between the nearest neighbour vibronic levels belonging to the same PEC are shown for comparison. From these considerations it can be expected that the relative strength of the interaction with phonons varies greatly among different vibronic lines and that the phonon effects will be expressed accordingly. At first sight one would assume that the lowest energy phonons give the largest contribution due to the reciprocal dependence. Although important, the number of phonons responsible for each such transition also plays a role. As the number of low-energy phonons is small (see Figure 2), the actual contribution is small as well. This can mathematically be understood, as in Eq. (15) the value of the function $g_\nu(t)$ depends on the energy difference between vibronic levels but also on the function υ^2.

3.2 Manifestations of phonons in spectra

In Figure 4 the calculated spectra of absorption and REPs for first- and second-order Raman scattering are presented (for the code of the calculations, see Appendix B.1).

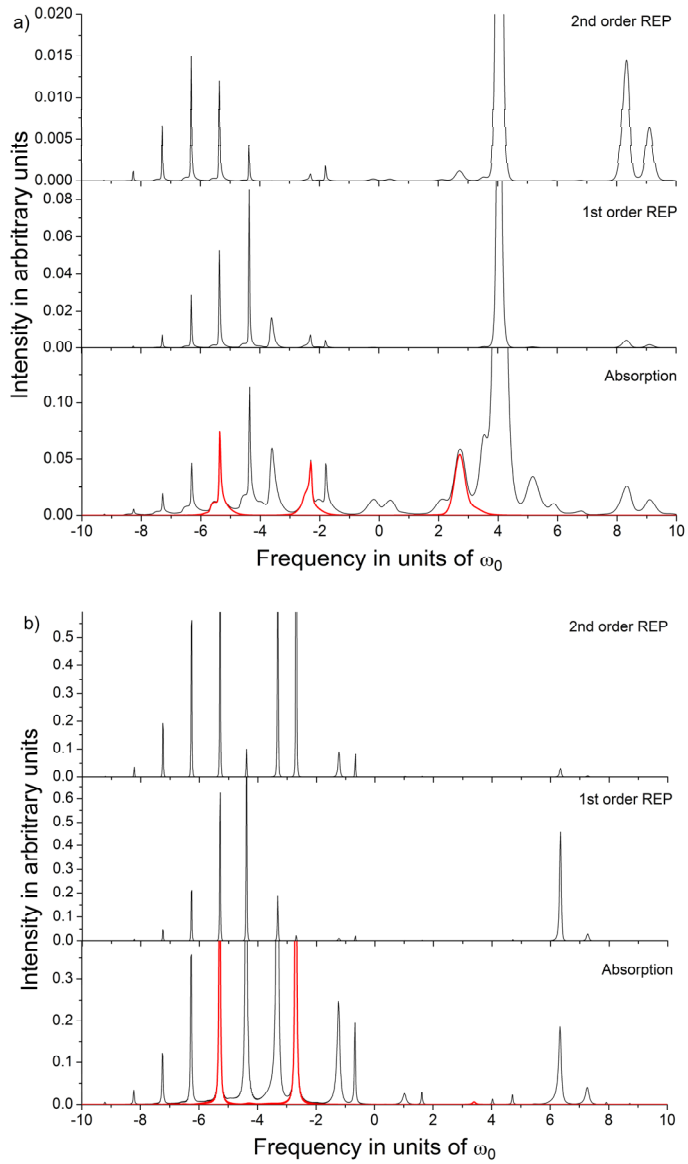

Figure 4. Absorption spectra and first- and second-order Raman excitation profiles for a) upper PEC b) lower PEC. Red lines (corresponding to $\nu = 5$, $\nu = 8$ and $\nu = 13$) highlight some vibronic lines and their phonon wings in the absorption spectra ($G = 3$, $D = 10$).

From these results the following observations can be made. Firstly, the distance between the vibronic lines is not equidistant. Although the starting point was the harmonic oscillator with its equidistant energy levels, the interaction with the main mode leads to a different system. Further more, different interaction strengths with phonons induce different shifts in the position of the lines. The spectrum can be divided into two parts: the + and – part, associated with the upper and the lower PEC, respectively (for the scale of the most intensive lines see the full spectrum in Figure 8). The transitions to both states have a distinct region. Due to the Franck-Condon principle the region lies near the point of quasi-degeneracy. The greatest overlap of wave functions with the upper energy curve in that region is with lower vibronic levels. There is a tendency that the first line is the most intensive and the intensity of other lines drops as one moves away from the point of quasi-degeneracy – a result similar to the transitions between two harmonic oscillators. This result is more observable in a strong interaction in Figure 5. The vibronic energy levels associated with a steep energy curve in harmonic approximation would be distantly spaced. The intensive lines of the upper PEC exhibit such behaviour. However, due to the interaction between the two PECs, there are also less intensive intermediate vibronic states. This result is an analogy of the Slonczewski resonances [22] observed in JT systems. For the PJTE this result had been obtained by Loorits [15]. The so-called Loorits resonances can also be seen from Figure 3. The energy difference between the next-neighbouring levels shows a periodic pattern coinciding with the positions of resonant vibronic lines. The reason for this is the correction to the position of the energy levels by vibronic interaction. Periodicity is the result of the repulsion of the energy levels of the lower PEC by the energy levels of the upper PEC.

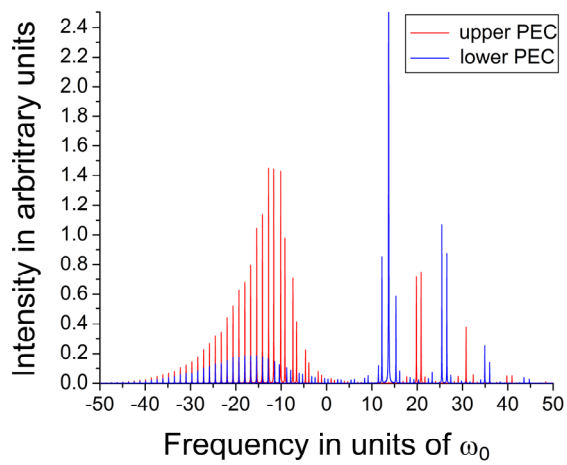

Figure 5. Absorption spectrum in the case of a strong vibronic interaction without the phonon contribution. The intensive lines for the upper potential form closely-packed groups and are the result of Loorits resonances ($G = 10$, $D = 300$).

For the lower energy curve the greatest overlap is with some intermediate states. The result is a broad region of continuously varying lines in the spectrum. Due to the mixing of the states the previous statements are a bit ambiguous, since there are excitations outside the main region of each PEC brought about by the interacting vibrational mode. Even the failure of the PEC interpretation becomes apparent, as there are excitations into the energy region below the concavity of the upper potential where one would not expect energy levels to be present. However, this is only the limit of using the present treatment for explaining complex quantum mechanical effects.

The novel results of this work are the finite (although small) widths of vibronic lines and the phonon wings accompanied with every vibronic line. It is worth emphasizing that each wing is unique, since the interaction strength of vibronic lines with the phonon bulk varies. It can be seen that some lines have hardly any phonon wings (sharp lines in 4b) when some lines have disappeared and their energy has been completely transferred to the phonon wing (broad bands in 4a).

The REPs provide additional information about phonon effects. The Raman active frequencies in the excitation profiles are associated with different active vibrational modes. However, the Raman spectra have their own peculiarities. Due to quantum-mechanical interference effects some lines may be absent from the spectra or have essentially diminished values.

3.3 Special case of soft dynamics

A special case of soft dynamics was discussed in papers [II], [III]. In the soft dynamics case the lower energy curve is flat (Figure 6) and the theory can be tested against other predictions. The most important addition to the theory was the inclusion of the frequency change into calculations. If one would look at a transition from a ground state with a frequency larger than that of the excited state, then the PEC of the excited state would be flatter as compared to the PEC of the ground state. The inclusion of the PJTE makes the curve practically constant over the entire region of configurational coordinates where one would expect excitations to occur (Figure 6).

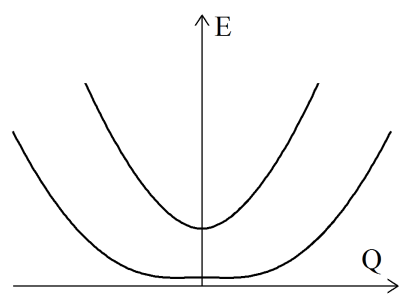

Figure 6. Qualitative shape of the potential energy curves of the excited state in the case of soft dynamics ($G = 20$, $D = 3$)

The zero-point energy of the lower PEC is very small and the vibronic levels are very close together in the region where the ground PEC has a significant overlap with the lower branch of the excited state. The first conclusion is that the absorption lines corresponding to the transitions to different vibronic levels almost coincide. This means that the vibronic states of the excited states are almost with the same energy. The second one is that the kinetic energy of the initial ground state has a large contribution to the spectrum of the absorption band. Namely, the transitions corresponding to the different values of the configurational coordinate have different kinetic energy values and, due to the conservation of energy and the coincidence of the excited energy levels, the kinetic energy will be deduced from the energy required for the transition. The independent prediction discussed in [II] is that the shape of the absorption band in the excitation to the lowest levels of the lower PEC is lambda-shaped. The line width should be in the order of the quanta of the ground state. The calculations of the current theory support this prediction as can be seen from the envelope of the lines in Figure 7. The frequency of the ground state was taken to be $4\omega_0$, so the entire spectrum is within two quanta of the ground state vibrations.

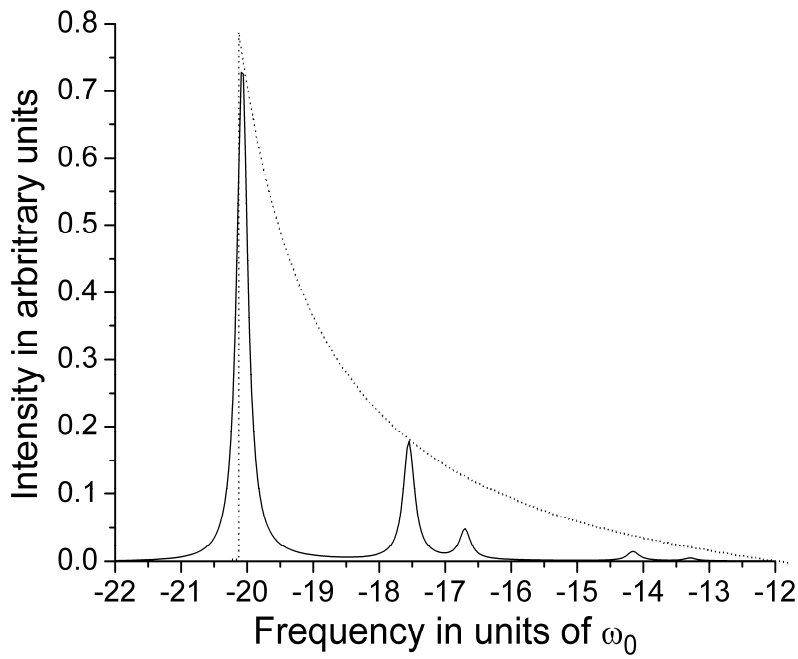

Figure 7. Lambda shape of the convolution of the low energy part of the lower potential energy curve in the case of soft dynamics ($G = 20$, $D = 3$).

The effects of the frequency change can also be seen in the spectra for other PJTE cases. In these cases the shape of the ground state determines the probability of the exciting vibronic states of the upper or lower PEC. In other words, the overlap of the wave functions changes especially in the case when the frequency of the ground state is large, the corresponding PEC is steep and the probability of the exciting vibronic states of the lower PEC of the excited state becomes smaller. This can be seen if one will compare the spectra in Figure 8. All the other parameters of the calculations were kept the same, but the changes in the intensity of the lines can be seen. As expected, the lines at larger values of the configurational coordinate lose intensity, while the ones near the origin gain intensity (become more probable).

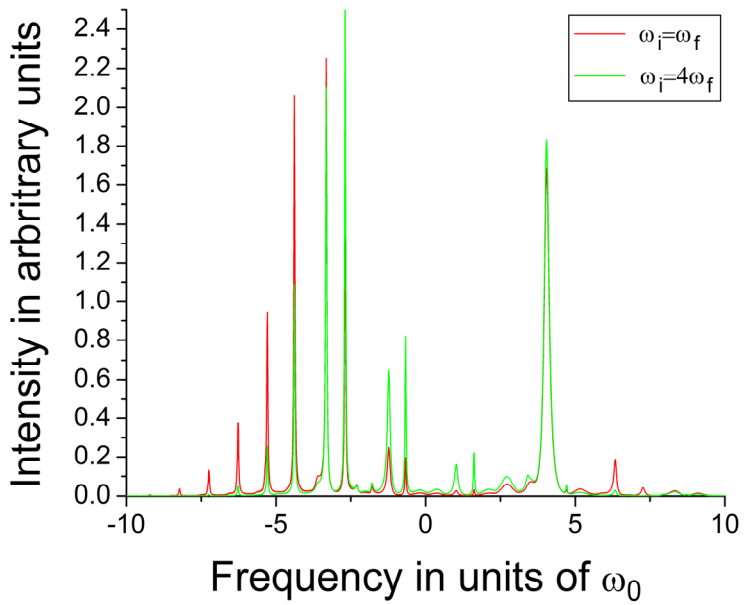

Figure 8. Absorption spectrum in the case of frequency change during the excitation. The spectrum without frequency change (red) and the spectrum in the case when initial frequency is four times larger than in the final state (green) ($G = 3$, $D = 10$).

4. RELAXATION

To calculate the relaxation of any quantity in the excited state the formalism of the density operator of the vibronic subsystem $\hat{\rho}$ is applied. This operator is defined as follows:

$$\hat{\rho}^{\pm} = \sum_{\nu\nu'} \left\langle 0_{ph} \left| e^{-itH_e} \right| \nu_{\pm} \right\rangle \left\langle \nu'_{\pm} \left| e^{itH_e} \right| 0_{ph} \right\rangle . \tag{25}$$

This definition assumes the zero temperature limit. The time dependence of the quantity A of the subsystem can be presented as $A(t) = Tr\left(\hat{A}\hat{\rho}^{\pm}(t) \right)$. Below the superscripts are omitted. The calculations of $\hat{\rho}^{+}$ and $\hat{\rho}^{-}$ can be made analogously. The time derivative for the matrix elements of Eq. (25) can be presented as (see Appendix A.6)

$$\dot{\rho}_{\nu\nu'}(t) = -i\omega_{\nu\nu'}\rho_{\nu\nu'}(t) + \lambda^2 \int_0^t d\tau\, G(\tau) \sum_{\nu_1\nu_1'} A_{\nu\nu_1} \left(\rho_{\nu_1\nu_1'}(t-\tau) A_{\nu'\nu_1'} - A_{\nu_1'\nu_1} \rho_{\nu_1'\nu'}(t-\tau) \right) e^{i\omega_{\nu'\nu_1'}\tau} + Hc , \tag{26}$$

where $\omega_{\nu\nu'} = E_{\nu}^{+} - E_{\nu'}^{-}$ is the energy difference of the states $\left| \nu_{+} \right\rangle$ and $\left| \nu'_{-} \right\rangle$,

$$A_{\nu\nu'} = \left\langle \nu_{+} \left| a^{+} \right| \nu'_{-} \right\rangle = \sum_{n} \sqrt{n+1} C_{\nu n}^{+} C_{\nu' n+1}^{-} \tag{27}$$

and the correlation function $G(\tau) = \sum_{j\geq 1} \upsilon_j^2 \left\langle 0_{ph} \left| a_j(t) a_j^{+}(t') \right| 0_{ph} \right\rangle = \sum_{j\geq 1} \upsilon_j^2 e^{-i\omega_j \tau}$ describes the phonon excitations.

Eq. (26) must be solved by using the initial condition. Note that in the large time limit one can take $\rho(t-\tau) \approx \rho(t)$. In this approximation Eq. (26) reduces to the master equation in the Lindblad form [23].

In the case of a strong vibronic coupling with the main mode and weak coupling with phonons then the time dependence of the diagonal and non-diagonal elements of the density matrix is different. The non-diagonal elements change very fast in time with the characteristic reciprocal time $\sim \sqrt{D}\,\omega_0$, where $D \gg 1$. The time-dependence of the diagonal elements, however, is determined only by the interaction with phonons, which in our case is considered to be weak; the corresponding characteristic reciprocal time is at least λ^2 times smaller than $\sqrt{D}\,\omega_0$.

4.1 Diagonal elements of the density matrix

The density matrix gives two types of information. The non-diagonal elements describe the dephasing of the initial wave packet and are of no interest at the moment, since this process is very fast and the energy of the system remains the same (also, this has been previously studied [24]). The diagonal elements $\rho_{\nu\nu}$, however, describe the population of the vibronic levels and are of special interest, since the electron transfer from one vibronic level to another has to be accompanied by an energy transfer. As the energy difference of the vibronic lines is small, this cannot be done by radiation. The way for the system to lose energy is by creating vibrations in the crystal or through less probable second-order processes.

Neglecting the fast oscillating terms under the integral in Eq. (26) and taking into account that $\rho(t-\tau) \approx \rho(t)$, one gets

$$\dot{\rho}_{\nu\nu} \approx -\gamma_\nu \rho_{\nu\nu} + \lambda^2 \sum_{\nu' \neq \nu} A^2_{\nu'\nu} \int_{-t}^{t} d\tau G(\tau) \rho_{\nu'\nu'}(t-\tau) e^{i\omega_{\nu'\nu}t} . \quad (28)$$

The phonon correlation function $G(\tau)$ differs from zero essentially only for $\tau \leq t_0$, where t_0^{-1} is the characteristic width of the phonon spectrum. Therefore, for $t \gg t_0$ Eq. (28) is reduced to the standard kinetic equation

$$\dot{\rho}_{\nu\nu} \approx -\gamma_\nu \rho_{\nu\nu} + \sum_{\nu' \neq \nu} \gamma_{\nu'\nu} \rho_{\nu'\nu'} , \quad (29)$$

where

$$\gamma_\nu = \sum_{\nu'} \gamma_{\nu\nu'} , \quad (30)$$

$$\gamma_{\nu'\nu} = \lambda^2 A^2_{\nu'\nu} \int_{-t}^{t} d\tau G(\tau) e^{i\omega_{\nu'\nu}t} . \quad (31)$$

The first term in the right-hand side of Eq. (29) describes the rate of the decay of the level ν due to the phonon-assisted transitions from this level to the other levels, the second term describes the transitions from all other levels to the level ν.

4.2 Dynamics of the configurational coordinate

Depending on experimental conditions, namely with a linearly polarized white laser pulse, two states, described respectively by $\rho^+_{\nu\nu'}$ and $\rho^-_{\nu\nu'}$, may be excited with the initial value

$$\rho^\pm_{\nu\nu'}(0) = C^\pm_{0\nu} C^\pm_{0\nu'} . \quad (32)$$

The distribution function of the state + at time *t* is given by the equation

$$P^{+}(Q,t)=\sum_{\nu\nu'}\Psi_{\nu}^{+}(Q)\Psi_{\nu'}^{+}(Q)\rho_{\nu\nu'}^{+}(t)\,, \tag{33}$$

where

$$\Psi_{\nu}^{+}(Q)=\sum_{n}C_{2n\nu}^{+}\psi_{2n}(Q) \tag{34}$$

is the wave function of the state ν_{+} in a coordinate representation (the distribution function $P^{-}(Q,t)$ can be found analogously). In the case of PJTE $\psi_{n}(Q)$ are the eigenfunctions of the harmonic oscillator:

$$\psi_{n}(Q)=\sqrt{\frac{1}{2^{n}n!}}\left(\frac{\omega_{0}}{\pi}\right)^{1/4}e^{-\omega_{0}Q^{2}/2}H_{n}\left(\sqrt{\omega_{0}}\,Q\right), \tag{35}$$

where $H_{n}\left(x\right)$ is the Hermite polynomial. In the slow energy relaxation stage $\rho_{\nu\nu'}^{\pm}(t)\approx\rho_{\nu\nu'}(t)\,\delta_{\nu\nu'}$ and

$$P^{\pm}(Q,t)\approx\sum_{\nu}\rho_{\nu\nu}(t)\,\Psi_{\nu}^{\pm 2}(Q)\,. \tag{36}$$

The function $P^{\pm}(Q,t)$ can be calculated by solving the kinetic equation Eq. (29) by using the initial condition of Eq. (32). The results of these calculations are presented below (for the code of the calculations see Appendix B.2).

Since the short-time relaxation is not in the scope of this discussion, the initial allocation of the distribution function is taken to be already dephased. Without dephasing the distribution function should be (at least in the beginning of the process) a Gaussian of the ground state of a harmonic oscillator. Figure 9 b,d exhibits a clear delocalization. The maximum centred at the origin is the result of an excitation from the ground state to the upper potential. The regions away from the origin are related to the lower energy curve. As expected, the interaction strength determines the shape of the PECs and influences the probability of exciting the states of the upper or lower PEC. The actual relaxation can also play a role. A stronger vibronic coupling results in a stronger mixing of the two excited states. This implies a higher rate of the energy transfer from the central region associated with the upper energy curve to the lower energy curve, although the wave function overlap can still be significant.

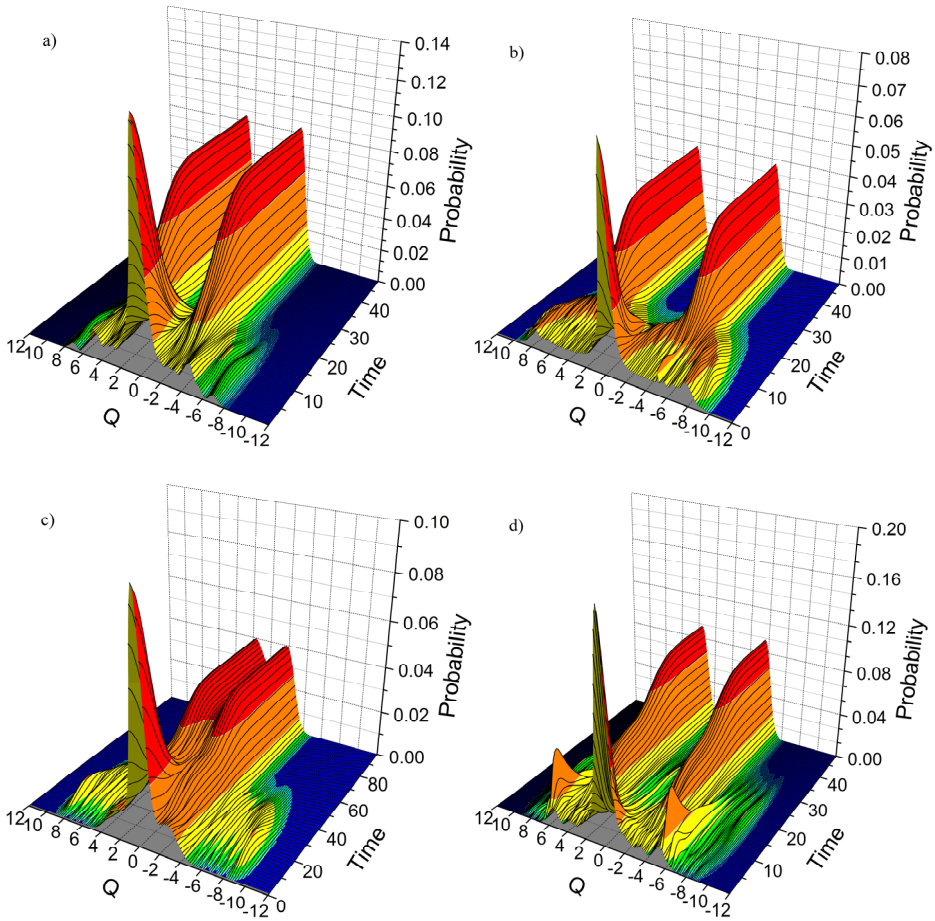

Figure 9. Relaxation of the configurational coordinate in the case of a) $G = 3$, $D = 5$ b) $G = 3, D = 10$ c) $G = 9, D = 6$ and d) $G = 9, D = 9$

One can see that the results are reasonable. The system relaxes to the two minima of the lower PEC. The increase of the parameter G (splitting of the states) separates the final states better and the increase in the vibronic coupling strength D produces more structure. In Figure 9 b,c there is an additional hint to the shape of the lower PEC. The system gradually loses intensity in the larger values of the configurational coordinate and the probability shifts towards the origin, which can be interpreted as the system's relaxation on the edges of the parabolic PEC. Figure 9 a and d do not show such clear tendency, which implies that the relaxation goes quickly from higher states through the intermediate states into the two minima. In Figure 9 c,d the non uniform decay of each vibronic line can be seen, as the incline of the two final maxima is not constant. To generalize, the relaxation seems to be faster in lower vibronic

levels and slower in higher levels near and above the quasi-degeneracy. In other words, the high-amplitude vibrations of the lower potential (wings at larger values of Q) do not initially decay before an additional energy is transferred from the upper potential (associated with the central maximum), however, at the end they disappear suddenly.

A different initial condition, the one where only one vibronic state is populated, corresponding to a theoretical case of spectrally selective quasi-monochromatic short light pulse, reinforces the conclusions made (in Figure 10).

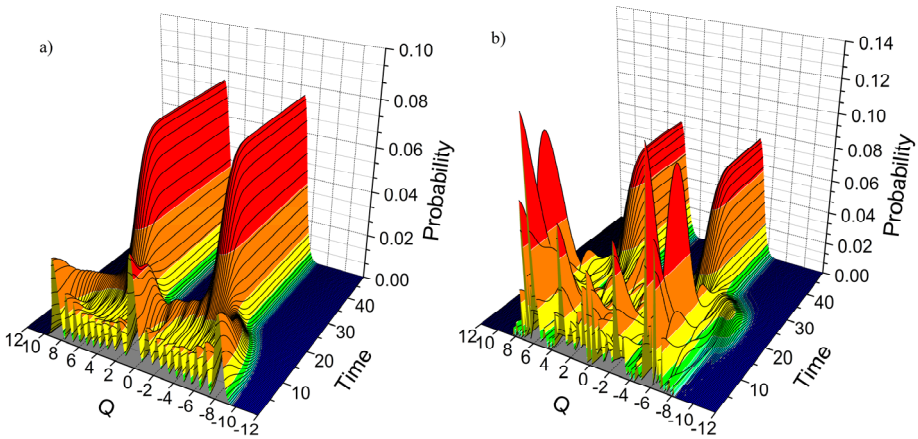

Figure 10. Relaxation of a configurational coordinate in the case of a quasi-monochromatic short light pulse. Here $G = 3$, $D = 10$ but the initial excited level differs: a) $\nu = 10$ b) $\nu = 30$

This time the initial probability distribution is determined by the wave function of the excited vibronic state. The wave function structure can be seen better and thus the excited vibronic lines can be distinguished (the appearance and disappearance of small “hills”).

5. DISCUSSION

This thesis gives a rigorous quantum-mechanical description of quasi-degenerate electronic states in a strong vibronic interaction with one vibrational mode and in a weaker interaction with all other bath modes. Bath modes play an important role in optical spectra as well as in the relaxation process.

The results of the study of the optical spectra of a PJTE system add an interesting feature to the discussion – the phonon wings in the absorption. The phonon wings can be used to determine the strength of the phonon interaction, keeping in mind that phonon wings are very different for different vibronic lines. This effect can also explain the absence of some lines in the spectra. The Raman spectra give a complementary and additional information about vibronic effects, namely the Raman active modes and their intensities.

The calculations of the non-radiative relaxation of energy, mediated by phonons in a strongly-excited quasi-degenerate electronic state of a dimer, has provided an insight into the complex processes involved. In this study it was done for a symmetric inital state. However, this approach can be straightforwardly extended for describing the relaxation of other initial states, including the ones corresponding to a system initially localized near an arbitrary point of the excited potential surface. The solution of such a problem would be important for a fully quantum-mechanical description of photochemical and other reactions of molecules in liquid solutions and in solids.

5.1 Limits and further research

In the course of developing the presented results some simplifications and assumptions were made that set a limit to the applicability of the theory. The first assumption was that the vibronic coupling in Eq. (3) can be treated in linear approximation. Many systems are described very well by linear approximation and the current theory has its applications. It is also possible to expand the current theory to include the quadratic coupling term, the difference being that the simple three diagonal matrices in Eq. (12) will be replaced by more complex ones.

In Eq. (4) an assumption was made that there existed one main mode through which the electronic states are coupled and the rest of the modes give only a small contribution. This was represented by the small dimensionless parameter λ. If this assumption does not hold, then the approximation in Eq. (6), where the λ^2 parameters were neglected, does not hold very well. The theory can be modified by taking into account more than one main mode. Again, the matrices in Eq. (12) are modified in the process. Strongly interacting modes should be excluded from the phonon spectrum up to the point where the contribution of the bulk is by the order of a magnitude smaller.

In the course of the development of the theory the zero temperature was assumed (Eq. (22) and Eq. (25)). The two main reasons for using such limit

were the ease of the development of the theory and the more clearer manifestation of phonon effects. This is not a major restriction, as the near-zero temperatures are experimentally achievable and the theory can be modified to take into account the finite temperatures. In the latter case the initial vibrational states should be expanded as $|i\rangle = \frac{1}{kT}\sum_n |n\rangle e^{-\frac{E_n}{kT}}$, where kT is the average thermal energy. However, a number of small effects may be lost due to the thermal broadening of lines.

The results of this model depend greatly on the model of the phonon density of states. The Debye-Van Hove model was used in this work, as this has a simple analytical form and it represents well the acoustic phonons. However, no restrictions apply to the choice of the model. For practical applications the phonon spectrum has to be calculated, for example, from the density functional theory.

SUMMARY

The theoretical model under observation was a quasi-degenerate electronic state in interaction via a nuclear displacement. This kind of vibronic interaction leads to a spontaneous symmetry breaking in the system and the phenomenon is called the pseudo Jahn-Teller effect. This thesis aims at giving a rigorous quantum-mechanical description of quasi-degenerate electronic states in a strong vibronic interaction with one vibrational mode and in a weaker interaction with all other bath modes. This system is characterized by large non-adiabaticity, which was taken into account. The model in question could describe a molecule or an impurity centre in solid. So far there has been no satisfactory description of such systems. The emphasis has been on the methods that take into account the single modes which describe molecules in a gaseous environment or a large number of phonons has been taken into account only approximately.

The optical spectra of the systems mentioned were among the results achieved in the course of the work. The theory was also expanded to include the calculation of relaxation. The main idea was to rewrite the Hamiltonian of the system in the coordinates where an additional quadratic potential energy term of vibrations describes the interaction of the main mode and the rest of phonons. The latter interaction was taken into account approximately by using the methods from the field theory. After representing these relations on a suitable basis, it was possible to solve the eigenvalue problem numerically. These numeric results were used to describe the rest of the system. To such parameters belonged the lifetimes of vibronic states that were used to find the relaxation of the system. To that effect the density matrix was used. The time evolution of the density matrix can be found by solving the corresponding master equation. The time-dependent density matrix can then be used to describe the evolution of any quantum mechanical quantity.

The results obtained are unique, since they give an insight into the process involved near the region of quasi-degeneracy. The phonon wings can clearly be seen in the optical spectra and their intensity is greatly dependent on the interaction strength between the vibronic state and the phonon continuum. The same reason – the varying strength of the vibronic interaction – influences also the relaxation process. It is important to emphasize that the relaxation is non-radiative and the only way to transfer energy from the system to phonons is via vibronic interaction. The inclusion of the whole phonon spectrum was a novel result and this is the first accurate description of the relaxation of pseudo Jahn-Teller systems.

SUMMARY IN ESTONIAN

Mitteadiabaatilisuse arvestamine pseudo-Jahni-Telleri efektis: foononite mõju

Antud töö uurimisobjektiks on olnud teoreetiline süsteem, kus eksisteerib tuumakoordinaatide muutus, mis muudab kahte kvaasikõdunud elektroonset seisundit nii, et nad kattuvad. Need elektroonsed seisundid on seetõttu omavahel interaktsioonis läbi vibroonse interaktsiooni. See interaktsioon viib mainitud süsteemi iseenesliku sümmeetria rikkumiseni ning seda nähtust kutsutakse pseudo-Jahni-Telleri efektiks. Doktoritöö eesmärk on arendada välja puhtalt kvantmehaaniline teooria, mis on võimeline kirjeldama kvaasikõdunud elektroonseid seisundeid tugevas vibroonses interaktsioonis. Oluline on seejuures arvestamine suure hulga võnkemoodidega – foononitega. Sellist süsteemi iseloomustab tugev kõrvalekalle adiabaatilisest lähendist (mitteadiabaatilisus) elektronseisundite lõikumise piirkonnas, mida tuli arvesse võtta. Eelpool-kirjeldatud mudel võib realiseeruda molekuli või lisanditsentri korral kristallis. Seni ei ole sellist süsteemi suudetud rahuldava täpsusega kirjeldada. Keskendutud on meetoditele, mis arvestavad üksikuid võnkumisi, mis on piisav molekulide kirjeldamiseks gaasilises keskkonnas, või on suuremat hulka foononeid arvesse võetud vaid ligikaudselt.

Töö käigus saavutati tulemused, mis kirjeldavad mainitud süsteemide mudeli optilisi spektreid ning seda arendati edasi relaksatsiooni arvutamiseks. Põhiline lähenemise idee seisneb süsteemi hamiltoniaani ümberkirjutamises koordinaatides, kus peamine elektronseisundite interaktsioon toimub läbi peamise võnkumiste moodi ja interaktsiooni ülejäänud foononitega on arvesse võetud ligikaudselt väljateooria meetodeid kasutades. Kirjeldades neid seoseid sobivas baasis on numbriliselt võimalik leida vastava omaväärtusvõrrandi lahendid. Neid numbrilisi tulemusi on edaspidi võimalik kasutada ülejäänud süsteemi kirjeldamisel. Relaksatsiooni arvestamiseks oli võimalik kasutada võnkeseisundite leitud eluigasid, mis võimaldavad kirja panna süsteemi iseloomustava tihedusmaatriksi. Tihedusmaatriksi ajaline evolutsioon on võimalik leida kineetilise võrrandi abil. Ajast sõltuvat tihedusmaatriksit on omakorda võimalik kasutada suvalise kvantmehaanilise suuruse leidmiseks ning seega ka nende suuruste ajalise evolutsiooni leidmiseks.

Saadud tulemused on huvipakkuvad, sest välditud koonilise lõikumise piirkonnas on süsteemil mittetriviaalne käitumine. Optilistes spektrites on näha selge foononite mõju foonontiibade näol. Foonontiibade intensiivsus aga sõltub väga tugevalt konkreetse joone interaktsiooni tugevusest võnkumistega ning seega on samas spektris näha väga erinevate foonontiibadega spektrijooni. Sama põhjus – erinev interaktsioon võnkumistega – mõjutab ka relaksatsiooniprotsessi. Oluline on mainida, et relaksatsiooniprotsessi käigus ei eraldu energiat footonitena ehk tegemist on mitteradiatiivse protsessiga. Ainuke võimalik viis energiat ära anda on foononinteraktsiooni kaudu võre võnkumistele. Foononeid ei olnud suudetud suurel hulgal varasemates töödes avesse võtta, mis tähendab, et ka selliste süsteemide relaksatsiooni ei olnud varasemalt täpselt kirjeldatud.

Appendix A: Derivations of some equations

A.1 Transformation of the Hamiltonian of the system into a new basis

The following definitions are used:

$$Q = \left(1+\lambda^2\right)^{-1/2}\left(x_0 + \lambda q_1\right),$$

$$Q_l = \left(1+\lambda^2\right)^{-1/2}\left(q_l - \lambda x_0\right),$$

where $q_l = \sum_{j\geq 1} e_{lj} x_j$, $\sum_j e_{lj}^2 = 1$.

The back transformation is

$$x_0 = \left(1+\lambda^2\right)^{-1/2}\left(Q - \lambda Q_1\right),$$

$$q_l = \left(1+\lambda^2\right)^{-1/2}\left(Q_l + \lambda Q\right).$$

Since all the definitions are mutually orthogonal, they do not change the shape of the kinetic part of the Hamiltonian $H_g = \frac{1}{2}\sum_j \left(-\frac{\partial^2}{\partial x_j^2} + \omega_j^2 x_j^2 \right)$. After separating the main contributing mode the potential part can be transformed by using the definitions.

$$\omega_j^2 x_j^2 = \omega_0^2 x_0^2 + \sum_{j\geq 1} \omega_j^2 x_j^2 = \omega_0^2 x_0^2 + \sum_{l\geq 1}\sum_{l'\geq 1} D_{ll'} q_l q_{l'} =$$

$$= \left(1+\lambda^2\right)^{-1}\left(\omega_0^2\left(Q^2 - 2\lambda Q Q_1 + \lambda^2 Q_1^2\right) + \left(\sum_{l\geq 1}\sum_{l'\geq 1} D_{ll'} Q_l Q_{l'} + 2\lambda Q \sum_{l\geq 1} D_{1l} Q_l + \lambda^2 Q^2 \right)\right) =$$

$$= \left(1+\lambda^2\right)^{-1}\left(\omega_0^2 Q^2 + \sum_{l\geq 1}\sum_{l'\geq 1} D_{ll'} Q_l Q_{l'} - 2\lambda Q\left(\omega_0^2 Q_1 - \sum_{l\geq 1} D_{1l} Q_l \right) + \left(\lambda^2 \omega_0^2 Q_1^2 + \lambda^2 \omega_j^2 Q^2 \right)\right).$$

If one retains all the terms with powers of λ less than 2, takes $\left(1+\lambda^2\right)^{-1} \approx 1$ and considers that in the last term $Q_l \approx \sum_{j\geq 1} e_{lj} x_j$ (other contributions are also in the order of λ^2), the potential energy becomes

$$\omega_0^2 Q^2 + \sum_{l\geq 1}\sum_{l'\geq 1} D_{ll'} Q_l Q_{l'} - 2\lambda Q\left(\omega_0^2 Q_1 - \sum_{l\geq 1} D_{1l} Q_l\right) = \omega_0^2 Q^2 + \sum_{l\geq 1}\sum_{l'\geq 1} D_{ll'} Q_l Q_{l'} - 2\lambda Q\left(\omega_0^2 \sum_{j\geq 1} e_{1j} x_j - \sum_{l\geq 1} D_{1l} \sum_{j\geq 1} e_{lj} x_j\right) =$$
$$= \omega_0^2 Q^2 + \sum_{l\geq 1}\sum_{l'\geq 1} D_{ll'} Q_l Q_{l'} - 2\lambda \sum_{j\geq 1} e_{1j} Q\left(\omega_0^2 - \omega_j^2\right) x_j.$$

The relation $\sum_{l\geq 1} D_{1l} e_{lj} = \omega_j^2 e_{1j}$ was used in the last part. Considering the obtained result in writing the Hamiltonian of the system and by using the ladder operators (up to a constant), one gets

$$H_g = \frac{1}{2}\sum_j\left(-\frac{\partial^2}{\partial x_j^2} + \omega_j^2 x_j^2\right) \approx \frac{1}{2}\left[\left(-\frac{\partial^2}{\partial Q^2} + \omega_0^2 Q^2\right) + \left(-\sum_{j\geq 1}\frac{\partial^2}{\partial x_j^2} + \sum_{j\geq 1}\omega_j^2 x_j^2\right) - 2\lambda\sum_{j\geq 1} e_{1j} Q\left(\omega_0^2 - \omega_j^2\right) x_j\right] \approx$$
$$\approx \omega_0\, a_0^+ a_0 + \sum_{j\geq 1}\omega_j\, a_j^+ a_j + \lambda\sum_{j\geq 1} e_{1j}\left(\omega_0^2 - \omega_j^2\right)\frac{\left(a_0^+ + a_0\right)}{\sqrt{2\omega_0}}\frac{\left(a_j + a_j^+\right)}{\sqrt{2\omega_j}} = H_0 + H_{ph} + H'.$$

A.2 Derivation of three diagonal forms of the vibronic Hamiltonian

Starting with the vibronic Hamiltonian

$$(H_0 \cdot I + V)\begin{pmatrix}|\nu_+\rangle\\ |\nu_-\rangle\end{pmatrix} = E_\nu \begin{pmatrix}|\nu_+\rangle\\ |\nu_-\rangle\end{pmatrix}.$$

Substituting $H_0 = \omega_0\, a_0^+ a_0$, $V = \begin{pmatrix} G & \sqrt{D}\left(a_0 + a_0^+\right)\\ \sqrt{D}\left(a_0 + a_0^+\right) & -G\end{pmatrix}$ and

$E_\nu = \omega_0 \nu$ ($\hbar = 1$) and taking it in the units of ω_0 one gets

$$\begin{pmatrix} a_0^+ a_0 + G & \sqrt{D}\left(a_0 + a_0^+\right)\\ \sqrt{D}\left(a_0 + a_0^+\right) & a_0^+ a_0 - G\end{pmatrix}\begin{pmatrix}|\nu_+\rangle\\ |\nu_-\rangle\end{pmatrix} = \nu\begin{pmatrix}|\nu_+\rangle\\ |\nu_-\rangle\end{pmatrix}.$$

Expanding $|\nu_\pm\rangle = \sum_n C_{n\nu}^\pm |n\rangle$, the equation gets the form

$$\sum_n\left[\left(G + n - \nu_+\right)C_{n\nu}^+ |n\rangle + \left(\sqrt{D(n+1)}\,|n+1\rangle + \sqrt{Dn}\,|n-1\rangle\right)C_{n\nu}^-\right] = 0,$$
$$\sum_n\left[\left(-G + n - \nu_-\right)C_{n\nu}^- |n\rangle + \left(\sqrt{D(n+1)}\,|n+1\rangle + \sqrt{Dn}\,|n-1\rangle\right)C_{n\nu}^+\right] = 0.$$

The effect of ladder operators on these eigenstates has been taken into account

$$a^{+}a\left|n\right\rangle = n\left|n\right\rangle, \qquad a^{+}\left|n\right\rangle = \sqrt{n+1}\left|n+1\right\rangle \qquad \text{and} \qquad a\left|n\right\rangle = \sqrt{n}\left|n-1\right\rangle.$$

Multiplying the equations by the bra-vector $\left\langle k\right|$ and taking into account the orthonormality of the set of eigenstates $\left\langle k\middle|n\right\rangle = \delta_{kn}$, the equations become

$$\left(G+k\right)C^{+}_{k\nu} + \sqrt{D\,(k-1)}\,C^{-}_{(k-1)\nu} + \sqrt{D\,k}\,C^{-}_{(k+1)\nu} = \nu_{+}\,C^{+}_{k\nu},$$
$$\left(-G+k\right)C^{-}_{k\nu} + \sqrt{D\,(k-1)}\,C^{+}_{(k-1)\nu} + \sqrt{D\,k}\,C^{+}_{(k+1)\nu} = \nu_{-}\,C^{-}_{k\nu}.$$

These equations can be presented in the matrix form

$$\begin{pmatrix} G & \sqrt{D} & 0 & 0 & \ldots \\ \sqrt{D} & 1-G & \sqrt{2D} & 0 & \ldots \\ 0 & \sqrt{2D} & 2+G & \sqrt{3D} & \ldots \\ 0 & 0 & \sqrt{3D} & 3-G & \ldots \\ \ldots & \ldots & \ldots & \ldots & \ldots \end{pmatrix}\begin{pmatrix} C^{+}_{0\nu} \\ C^{-}_{1\nu} \\ C^{+}_{2\nu} \\ C^{-}_{3\nu} \\ \ldots \end{pmatrix} = \nu \begin{pmatrix} C^{+}_{0\nu} \\ C^{-}_{1\nu} \\ C^{+}_{2\nu} \\ C^{-}_{3\nu} \\ \ldots \end{pmatrix},$$

$$\begin{pmatrix} -G & \sqrt{D} & 0 & 0 & \ldots \\ \sqrt{D} & 1+G & \sqrt{2D} & 0 & \ldots \\ 0 & \sqrt{2D} & 2-G & \sqrt{3D} & \ldots \\ 0 & 0 & \sqrt{3D} & 3+G & \ldots \\ \ldots & \ldots & \ldots & \ldots & \ldots \end{pmatrix}\begin{pmatrix} C^{-}_{0\nu} \\ C^{+}_{1\nu} \\ C^{-}_{2\nu} \\ C^{+}_{3\nu} \\ \ldots \end{pmatrix} = \nu \begin{pmatrix} C^{-}_{0\nu} \\ C^{+}_{1\nu} \\ C^{-}_{2\nu} \\ C^{+}_{3\nu} \\ \ldots \end{pmatrix}.$$

From here the eigenvalues can be found and the vibronic wave function takes the form

$$\left|\nu_{\pm}\right\rangle = \sum_{n} C^{\pm}_{2n,\nu}\left|2n\right\rangle\left|e_1\right\rangle + C^{\mp}_{2n+1,\nu}\left|2n+1\right\rangle\left|e_2\right\rangle.$$

A.3 Derivation of the formula for the cumulant-generating function

The vibronic Hamiltonian can be rewritten as $H_g + V \approx H_0 + H_{ph} + H' + V =$

$= H_2 + H'$.

Using the Dyson equation for the evolution operator averaged over zero-point states $\langle 0|\exp\left(it\left(H_g + V\right)\right)|0\rangle \approx \langle 0|\exp\left(it\left(H_2 + H'\right)\right)|0\rangle = \langle 0|\hat{T}\exp\left[i\int_0^t d\tau H'(\tau)\right]e^{iH_2 t}|0\rangle$.

$\hat{T}$ is the time-ordering operator used, since the Dyson equation is only applicable to ordered exponents, $H'(\tau) = \exp(i\tau H_2)H'\exp(-i\tau H_2)$. Taking the wave function to be the product of the electronic and phonon wave functions and using the basis of the vibronic Hamiltonian for the electronic wave function, one obtains (for + states, - states can be found by interchanging the subscripts)

$$\langle 0|\hat{T}\exp\left[i\int_0^t d\tau H'(\tau)\right]e^{itH_2}|0\rangle = \langle 0|\langle 0_{ph}|\hat{T}\exp\left[i\int_0^t d\tau H'(\tau)\right]e^{itH_2}|0_{ph}\rangle|0\rangle =$$

$$= \sum_{\nu}\sum_{\nu'} C^{+}_{0\nu}C^{+}_{0\nu'}\langle \nu_+|\langle 0_{ph}|\hat{T}\exp\left[i\int_0^t d\tau H'(\tau)\right]e^{itH_2}|0_{ph}\rangle|\nu_+\rangle =$$

$$= \sum_{\nu}\sum_{\nu'} C^{+}_{0\nu}C^{+}_{0\nu'}e^{iE^{+}_{\nu}t}\langle \nu_+|\langle 0_{ph}|\hat{T}\exp\left[i\int_0^t d\tau H'(\tau)\right]|0_{ph}\rangle|\nu_+\rangle.$$

Using the cumulant expansion for the term $\langle \nu_+|\langle 0_{ph}|\hat{T}\exp\left[i\int_0^t d\tau H'(\tau)\right]|0_{ph}\rangle|\nu_+\rangle$ and taking only the first two cumulants into account, one gets for the moment generating function

$$g^{+}_{\nu}(t) \approx i\int_0^t d\tau\,\langle \nu_+|\langle 0_{ph}|H'(\tau)|0_{ph}\rangle|\nu_+\rangle - \int_0^t d\tau\int_0^{\tau} d\tau'\,\langle \nu_+|\langle 0_{ph}|H'(\tau)H'(\tau')|0_{ph}\rangle|\nu_+\rangle.$$

The first term represents the expectation value of the Hamiltonian H' and is zero in our case.

$$g_{\nu}^{+}(t)=-\int_0^t d\tau\int_0^{\tau} d\tau'\,\langle \nu_+|\langle 0_{ph}|H'(\tau)\sum_{\nu'}|\nu'_-\rangle\langle\nu'_-|H'(\tau')|0_{ph}\rangle|\nu_+\rangle=$$

$$=-\int_0^t d\tau\int_0^{\tau} d\tau'\,\langle \nu_+|\langle 0_{ph}|e^{iH_2 t}H'e^{-iH_2 t}\sum_{\nu'}|\nu'_-\rangle\langle\nu'_-|e^{iH_2 t}H'e^{-iH_2 t}|0_{ph}\rangle|\nu_+\rangle=$$

$$=-\int_0^t d\tau\int_0^{\tau} d\tau'\,e^{i\omega_j\tau}e^{iE_{\nu}^{+}\tau}e^{-iE_{\nu'}^{-}\tau}e^{-i\omega_j\tau'}e^{-iE_{\nu}^{+}\tau'}e^{iE_{\nu'}^{-}\tau'}\langle \nu_+|\langle 0_{ph}|H'\sum_{\nu'}|\nu'_-\rangle\langle\nu'_-|H'|0_{ph}\rangle|\nu_+\rangle=$$

$$=-\sum_{\nu'}\langle \nu_+|\langle 0_{ph}|H'|\nu'_-\rangle\langle\nu'_-|H'|0_{ph}\rangle|\nu_+\rangle\int_0^t d\tau\int_0^{\tau} d\tau'\,e^{i\left(E_{\nu}^{+}-E_{\nu'}^{-}+\omega_j\right)(\tau-\tau')}=$$

$$=\sum_{\nu'}\langle \nu_+|\langle 0_{ph}|H'|\nu'_-\rangle\langle\nu'_-|H'|0_{ph}\rangle|\nu_+\rangle\int_0^t d\tau\,\frac{1}{i\left(E_{\nu}^{+}-E_{\nu'}^{-}+\omega_j\right)}\left(1-e^{i\left(E_{\nu}^{+}-E_{\nu'}^{-}+\omega_j\right)\tau}\right)=$$

$$=\sum_{\nu'}\langle \nu_+|\langle 0_{ph}|H'|\nu'_-\rangle\langle\nu'_-|H'|0_{ph}\rangle|\nu_+\rangle\left(\frac{-it}{E_{\nu}^{+}-E_{\nu'}^{-}+\omega_j}+\frac{e^{i\left(E_{\nu}^{+}-E_{\nu'}^{-}+\omega_j\right)t}-1}{\left(E_{\nu}^{+}-E_{\nu'}^{-}+\omega_j\right)^2}\right).$$

Here

$$\langle\nu'_-|H'|0_{ph}\rangle|\nu_+\rangle=\langle\nu'_-|\lambda\sum_{j\geq 1}\upsilon_j\left(a_0^{+}+a_0\right)\left(a_j+a_j^{+}\right)|0_{ph}\rangle|\nu_+\rangle=$$

$$=\lambda\sum_{j\geq 1}\upsilon_j\langle\nu'_-|\left(a_0^{+}+a_0\right)|\nu_+\rangle\left(a_j+a_j^{+}\right)|0_{ph}\rangle=\lambda\sum_{j\geq 1}\upsilon_j S^{+}_{\nu\nu'}a_j^{+}|0_{ph}\rangle\,,$$

where

$$S^{+}_{\nu\nu'}=\langle\nu'_-|\left(a_0^{+}+a_0\right)|\nu_+\rangle=\left(\sum_{n'}C^{-}_{2n',\nu'}\langle 2n'|\langle e_1|+C^{+}_{2n'+1,\nu'}\langle 2n'+1|\langle e_2|\right)\left(a_0^{+}+a_0\right)\left(\sum_{n}C^{+}_{2n,\nu}|2n\rangle|e_1\rangle+C^{-}_{2n+1,\nu}|2n+1\rangle|e_2\rangle\right)=$$

$$=\sum_{n}\sum_{n'}C^{-}_{2n',\nu'}C^{+}_{2n,\nu}\langle e_1||e_1\rangle\langle 2n'|\left(a_0^{+}+a_0\right)|2n\rangle+C^{+}_{2n'+1,\nu'}C^{-}_{2n+1,\nu}\langle e_2||e_2\rangle\langle 2n'+1|\left(a_0^{+}+a_0\right)|2n+1\rangle=$$

$$=\sum_{n}\sum_{n'}C^{-}_{2n',\nu'}C^{+}_{2n,\nu}\left(\delta_{2n',2n+1}\sqrt{2n+1}+\delta_{2n',2n-1}\sqrt{2n}\right)+C^{+}_{2n'+1,\nu'}C^{-}_{2n+1,\nu}\left(\delta_{2n'+1,2n+2}\sqrt{2n+2}+\delta_{2n'+1,2n}\sqrt{2n+1}\right)=$$

$$=\sum_{n}\left(C^{-}_{2n+1,\nu'}C^{+}_{2n,\nu}\sqrt{2n+1}+C^{-}_{2n-1,\nu'}C^{+}_{2n,\nu}\sqrt{2n}+C^{+}_{2n+2,\nu'}C^{-}_{2n+1,\nu}\sqrt{2n+2}+C^{+}_{2n,\nu'}C^{-}_{2n+1,\nu}\sqrt{2n+1}\right)=$$

$$=\sum_{n}\left[C^{+}_{2n+1,\nu}\left(C^{-}_{2n,\nu'}\sqrt{2n+1}+C^{-}_{2n+2,\nu'}\sqrt{2n+2}\right)+C^{-}_{2n+1,\nu}\left(C^{+}_{2n,\nu'}\sqrt{2n+1}+C^{+}_{2n+2,\nu'}\sqrt{2n+2}\right)\right].$$

The identities $\langle e_1||e_2\rangle=\langle e_2||e_1\rangle=0$ and

$$\langle 2n'|\left(a_0^{+}+a_0\right)|2n\rangle=\langle 2n'||2n+1\rangle\sqrt{2n+1}+\langle 2n'||2n-1\rangle\sqrt{2n}=\delta_{2n',2n+1}\sqrt{2n+1}+\delta_{2n',2n-1}\sqrt{2n}$$

have been used. Analogously $\langle\nu_+|\langle 0_{ph}|H'|\nu'_-\rangle=\lambda\sum_{j\geq 1}\upsilon_j S^{+}_{\nu\nu'}\langle 0_{ph}|a_j$.

This leads to

$$g_\nu^+(t) = \sum_{\nu'} \lambda^2 \sum_{j\geq 1} \upsilon_j^2 \left|S_{\nu\nu'}^+\right|^2 \left\langle 0_{ph}\left| a_j a_j^+ \right| 0_{ph}\right\rangle \left(\frac{-it}{E_\nu^+ - E_\nu^- + \omega_j} + \frac{e^{i\left(E_\nu^+ - E_{\nu'}^- + \omega_j\right)t} - 1}{\left(E_\nu^+ - E_{\nu'}^- + \omega_j\right)^2} \right) =$$

$$= \lambda^2 \sum_{\nu'} \sum_{j\geq 1} \upsilon_j^2 \left|S_{\nu\nu'}^+\right|^2 \left(\frac{-it}{E_\nu^+ - E_{\nu'}^- + \omega_j} + \frac{e^{i\left(E_\nu^+ - E_{\nu'}^- + \omega_j\right)t} - 1}{\left(E_\nu^+ - E_{\nu'}^- + \omega_j\right)^2} \right).$$

The derivation for $g_\nu^-(t)$ is analogous, with the exception that all the subscripts + and – are interchanged.

A.4 Derivation of the frequency change

The derivation follows that of Pae in her bachelor thesis. The transition from an initial ground state with the eigenstates corresponding to $H_i \left|m\right\rangle_i = \omega_i \left(m + \frac{1}{2} \right) \left|m\right\rangle_i$ to final states with the eigenstates $H_f \left|n\right\rangle_f = \omega_f \left(n + \frac{1}{2} \right) \left|n\right\rangle_f$ is kept in mind. The eigenstates of the final state will be used to expand the ground state of the Hamiltonian H_i over the eigenstates of the Hamiltonian H_f,

$$\left|0\right\rangle_i = \sum_n s_{2n} \left|2n\right\rangle_e .$$

Looking at the generating function

$$f(t) = {}_i\left\langle 0 \left| \exp\left(it \left(H_f - \frac{\omega_f}{2} \right) \right) \right| 0 \right\rangle_i = \sum_n {}_i\left\langle 0 \left| \exp\left(it \left(H_f - \frac{\omega_f}{2} \right) \right) \right| 2n \right\rangle_f {}_f\left\langle 2n \middle| 0 \right\rangle_i =$$

$$= \sum_n {}_i\left\langle 0 \middle| 2n \right\rangle_f {}_f\left\langle 2n \middle| 0 \right\rangle_i e^{2i\omega_f n} = \sum_n s_{2n}^2 e^{2i\omega_f nt}.$$

According to Kubo ja Toyozawa the generating function is

$$f(t) = \frac{\frac{2\sqrt{\omega_i \omega_f}}{\omega_i + \omega_f}}{\sqrt{1 - \left(\frac{\omega_i - \omega_f}{\omega_i + \omega_f} \right)^2 e^{2i\omega_f t}}} .$$

After expanding it into a power series by using

$$\frac{1}{\sqrt{1-x}} = \sum_{n=0}^{\infty} \frac{(2n-1)!!}{2^n n!} x^n ,$$

$$f(t) = \sum_n \frac{2\sqrt{\omega_i \omega_f}}{\omega_i + \omega_f} \frac{(2n-1)!!}{2^n n!} \left(\frac{\omega_i - \omega_f}{\omega_i + \omega_f} \right)^{2n} e^{2i\omega_f nt} .$$

If one would compare the two generating functions, then

$$s_{2n} = \sqrt{\frac{2(2n-1)!!\sqrt{\omega_i \omega_f}}{2^n n!(\omega_i + \omega_f)}} \left(\frac{\omega_i - \omega_f}{\omega_i + \omega_f} \right)^n .$$

A.5 Calculation of υ_j^2

The starting point is the definition of the function in Eq. (8)

$$\upsilon_j^2 = e_j^2 \left(\omega_0^2 - \omega_j^2 \right)^2 \Big/ 4\omega_0 \omega_j .$$

The normalized functions

$$\upsilon^2(\omega) = \sum_j \upsilon_j^2 \delta(\omega - \omega_j)$$

and

$$e^2(\omega) = \sum_j e_j^2 \delta(\omega - \omega_j)$$

can be introduced. In the low frequency limit $e_j^2 \propto \omega_j^2$ (long-wave acoustic vibration does not remarkably change the symmetric distances Q between the nearest atoms in the centre). Therefore,

$$e^2(\omega) = \frac{2}{\omega_M^2} \omega^2 \rho(\omega) = \frac{32\omega^4}{\pi \omega_M^6} \sqrt{\omega_M^2 - \omega^2} ,$$

$$\rho(\omega) = \frac{16}{\pi \omega_M^4} \omega^2 \sqrt{\omega_M^2 - \omega^2}$$

is the density of states of the acoustic phonons in the Debye-Van Hove model. ω_M is the maximum frequency of phonons. It follows that

$$\upsilon^2(\omega) = e^2(\omega)\frac{\left(\omega_0^2-\omega^2\right)^2}{4\omega_0\omega} = \frac{8\omega^3}{\pi\omega_0\omega_M^6}\left(\omega_0^2-\omega^2\right)^2\sqrt{\omega_M^2-\omega^2}\ .$$

A.6 Calculation of the density matrix elements

If one considers the time derivative, then $\dot{\tilde{\rho}} = -i\left\langle 0_{ph}\left|[\tilde{H}',\tilde{\rho}]\right|0_{ph}\right\rangle$. Up to the second order with respect to the interaction parameter λ it is given by the equation

$$\dot{\tilde{\rho}}(t) = -\lambda^2\int_0^t dt'\left\langle 0_{ph}\left|\left[\tilde{H}'(t),\left[\tilde{H}'(t'),\tilde{\rho}(t')\right]\right]\right|0_{ph}\right\rangle.$$

Here the Hamiltonian $H' = \lambda\sum_{j\geq 1}\upsilon_j\left(a_0^+ + a_0\right)\left(a_j + a_j^+\right)$ is used in the rotating wave approximation and the $a_0^+a_j^+$ and a_0a_j terms in the definition are neglected. The justification for such action is that the long-time relaxation conserves the energy of the system and the simultaneous creation or annihilation of the main mode and the phonons cannot have any large contribution. For further treatment one more observation has to be made. The operators $a_j(t)$ and $a_j^+(t)$ commute with $a_0(t)$, $a_0^+(t)$ and $\tilde{\rho}(t)$. Now if one considers the commutator $\left[\tilde{H}'(t),\left[\tilde{H}'(t'),\tilde{\rho}(t')\right]\right] = \tilde{H}'(t)\tilde{H}'(t')\tilde{\rho}(t') - \tilde{H}'(t)\tilde{\rho}(t')\tilde{H}'(t') - \tilde{H}'(t')\tilde{\rho}(t')\tilde{H}'(t) + \tilde{\rho}(t')\tilde{H}'(t')\tilde{H}'(t)$, then it is apparent that all the terms contain the product of the structure

$$\hat{A}\tilde{H}'(t)\hat{B}\tilde{H}'(t')\hat{C} = \hat{A}\left(a_0^+(t)a_j(t) + a_0(t)a_j^+(t)\right)\hat{B}\left(a_0^+(t')a_j(t') + a_0(t')a_j^+(t')\right)\hat{C} =$$

$$= \hat{A}a_0^+(t)\hat{B}a_0^+(t')\hat{C}a_j(t)a_j(t') + \hat{A}a_0(t)\hat{B}a_0^+(t')\hat{C}a_j^+(t)a_j(t') +$$

$$+\hat{A}a_0^+(t)\hat{B}a_0(t')\hat{C}a_j(t)a_j^+(t') + \hat{A}a_0(t)\hat{B}a_0(t')\hat{C}a_j^+(t)a_j^+(t').$$

Since $\left\langle 0_{ph}\left|a_j(t)a_j(t')\right|0_{ph}\right\rangle = \left\langle 0_{ph}\left|a_j^+(t)a_j(t')\right|0_{ph}\right\rangle = \left\langle 0_{ph}\left|a_j^+(t)a_j^+(t')\right|0_{ph}\right\rangle = 0$, only one term remains after the averaging.

$$\left\langle 0_{ph}\left|\left[\tilde{H}'(t),\left[\tilde{H}'(t'),\tilde{\rho}(t')\right]\right]\right|0_{ph}\right\rangle =$$

$$= \lambda^2\sum_{j\geq 1}\upsilon_j^2\left\langle 0_{ph}\left|a_j(t)a_j^+(t')\right|0_{ph}\right\rangle\left(a_0^+(t)a_0(t')\tilde{\rho}(t') - a_0^+(t)\tilde{\rho}(t')a_0(t') - a_0^+(t)\tilde{\rho}(t')a_0(t') + \tilde{\rho}(t')a_0^+(t)a_0(t')\right) =$$

$$= \lambda^2 G(t-t')\left[a_0^+(t)\left(a_0(t')\tilde{\rho}(t') - \tilde{\rho}(t')a_0(t')\right) - \left(a_0^+(t)\tilde{\rho}(t') - \tilde{\rho}(t')a_0^+(t)\right)a_0(t')\right].$$

Here

$$G(t-t') = \sum_{j\geq 1}\upsilon_j^2\left\langle 0_{ph}\left|a_j(t)a_j^+(t')\right|0_{ph}\right\rangle = \sum\nolimits_j \upsilon_j^2 e^{-i\omega_j(t-t')}\ .$$

The transformation to the Heisenberg representation is as follows:

$$\dot{\rho}(t) = i\left[H_2, \rho(t)\right] + e^{iH_2 t}\tilde{\rho}(t')e^{-iH_2 t}.$$

$$\dot{\rho}_{\nu\nu'}(t) = \left\langle \nu_+ \middle| \dot{\rho}(t) \middle| \nu'_+ \right\rangle = \left\langle \nu_+ \middle| i\left[H_2, \rho(t)\right] \middle| \nu'_+ \right\rangle + \left\langle \nu_+ \middle| e^{iH_2 t}\tilde{\rho}(t)e^{-iH_2 t} \middle| \nu'_+ \right\rangle =$$

$$= i\left(E_\nu^+ \rho_{\nu\nu'}(t) - E_{\nu'}^+ \rho_{\nu\nu'}(t)\right) + \lambda^2 \int_0^t dt' G(t-t') \cdot$$

$$\cdot \sum_{\nu_1\nu_1'} \left(A_{\nu\nu_1}\left(\rho_{\nu_1\nu_1'}(t')A_{\nu'\nu_1'} - A_{\nu_1'\nu_1}\rho_{\nu_1'\nu'}(t')\right)e^{i\omega_{\nu'\nu_1}(t-t')} + \left(\rho_{\nu\nu_1'}(t')A_{\nu_1\nu_1'} - A_{\nu\nu_1'}\rho_{\nu_1\nu_1'}(t')\right)A_{\nu_1'\nu'}e^{i\omega_{\nu'\nu_1}(t-t')}\right).$$

Here $\sum_{\nu_1}\left|\nu_{1-}\right\rangle\left\langle\nu_{1-}\right|$ and $\sum_{\nu_1'}\left|\nu'_{1-}\right\rangle\left\langle\nu'_{1-}\right|$ were inserted to get the terms $A_{\nu\nu'} = \left\langle \nu_+ \middle| a^+ \middle| \nu'_- \right\rangle = \sum_n \sqrt{n+1}C_{\nu n}^+ C_{\nu' n+1}^-$. $\omega_{\nu\nu'} = E_\nu^+ - E_{\nu'}^+$ is the energy difference of the states $\left|\nu'_+\right\rangle$ and $\left|\nu_+\right\rangle$.

Appendix B: MAPLE code for the calculations

B.1 Code for calculating optical spectra

```
> # MAPLE packages used by the program
with(LinearAlgebra):
with(DiscreteTransforms):

# Parameters of the calculation
Split:= 3;                              # Half splitting between
quasidegenerate states
Vibr:=10;                               # Vibrational coupling
strength
n := 1000;                              # Number of vibrational
levels to be calculated
N:= 2000;                               # Number of points that
determine the spectra
T:= 200;                                # Length of the spectrum
in time domain
g0:=0.02;                               # Parameter that
determines the line width from other effects
lambda := 0.03;                         # Constant that determines
the strength of phonon coupling
Om := 1.3;                              # Maximum frequency of
phonons
On := 1;                                # Frequency of the main
vibrational mode
Oi := 1;                                # Initial frequency
Of := 1;                                # Final frequency
Ips:=10**(-6);                          # Small constant for
avoiding singularities
nrstates := 25;                         # Number of vibrational
levels to be taken into account (higher levels will not be exited
and do not give any contribution)

# Variables of the claculation
A := Matrix(1..n,1..n, shape=symmetric ):   # Matrix of the
vibronic coupling
B := Matrix(1..n,1..n, shape=symmetric ):
rsu0 := Array(1..N,'datatype'='complex'[8]):# Fourier transform
of the spectra
rsu1 := Array(1..N,'datatype'='complex'[8]):
rsu2 := Array(1..N,'datatype'='complex'[8]):
rsl0 := Array(1..N,'datatype'='complex'[8]):
rsl1 := Array(1..N,'datatype'='complex'[8]):
rsl2 := Array(1..N,'datatype'='complex'[8]):
rsu := Matrix(1..nrstates,1..N):
```

```
rsl := Matrix(1..nrstates,1..N):

# Solving of the vibronic Hamiltonian
for i from 1 to n do                    # Initial setup of the
elements on the main diagonal
 A[i,i]:=(i-1) + ((-1)**(i-1))*Split :
 B[i,i]:=(i-1) + ((-1)**(i))*Split :
end do:

for s from 1 by 1 to (n-1) do           # Initial setup of the
off-diagonal elements
 A[s+1,s]:= evalf(sqrt (s*Vibr)) :
 B[s+1,s]:= evalf(sqrt (s*Vibr)) :
end do:

(Es,cs) := Eigenvectors(A):             # Solving the eigenvalue
problem
(Et,ct) := Eigenvectors(B):

for i from 1 by 2 to n-1 do             # Sorting of the
eigenvalues and eigenvectors associated with the upper and lower
potential
 Eu[i] := Es[i]:
 Eu[i+1] := Et[i+1]:
 El[i]:= Et[i]:
 El[i+1]:= Es[i+1]:

 for j from 1 to n do
  cu[i,j]:= cs[i,j]:
  cu[i+1,j]:= ct[i+1,j]:
  cl[i,j]:= ct[i,j]:
  cl[i+1,j]:= cs[i+1,j]:
 end do:
end do:

# Frequency change
for i from 0 by 1 to (n/2-1) do         # Calculation of
coefficients for the change of frequency
 s2n[i+1] :=
sqrt(2*sqrt(Oi*Of)/(Oi+Of))*sqrt(doublefactorial(2*i-
1)/(2**i*factorial(i)))*((Oi-Of)/(Oi+Of))**i:
end do:

for i from 1 to n do                    # Calculation of the
frequency-corrected eigenvectors of the vibronic coupling matrix
 Cu[i] := evalf(add( cu[2*k-1,i]*s2n[k], k = 1..n/2)) :
 Cl[i] := evalf(add( cl[2*k-1,i]*s2n[k], k = 1..n/2)) :
end do:
```

```
for i from 0 to 2 do                    # Calculation of the
vibronic correlation function
 for j from 1 to nrstates+1 do          # Since the maximum
frequency of phonons is fixed, only one vibrational level higher
and one lower are taken into account
  S[j,i+1]:=evalf(add( cu[2*k,j]*(sqrt(2*k-1)*cl[2*k-1,j+i]+
sqrt(2*k)*cl[2*k+1,j+i]) +
cl[2*k,j]*(sqrt(2*k-1)* cu[2*k-1,j+i]+ sqrt(2*k)* cu[2*k+1,j+i])
,  k = 1..n/2-1 )):
  S2[j,i+1]:=evalf(add( cl[2*k,j]*(sqrt(2*k-1)*cu[2*k-1,j+i]+
sqrt(2*k)*cu[2*k+1,j+i]) +
cu[2*k,j]*(sqrt(2*k-1)* cl[2*k-1,j+i]+ sqrt(2*k)* cl[2*k+1,j+i])
,  k = 1..n/2-1 )):
 end do:
end do:

for k from 1 by 1 to N do               # Points in time domain
where the spectrum is calculated
 times[k] := evalf((2*k-1-N)*T/(N-1)):
end do:

# Calculation of the cumulant-generating function
# First level outside of the main loop
for k from 1 to N do
 gma[1,1,k]:=0:
 gma2[1,1,k]:=0:
end do:
for i from 2 to 3 do
 for k from 1 to N do
  del:= Eu[1] - El[1+i-2];                          # Energy
difference between vibronic states
  gma[i,1,k]:=simplify(evalf(S[1,i]*S[1,i]*         # Cumulant-
generating function for +states
       lambda*
       Int(8*x**3*sqrt(Om**2-x**2)*
       (On**2-x**2)**2/
       (Pi*On*Om**6)*
    (exp(I*(del-x)*times[k])-1-I*times[k]*(del-x))/
       ((del-x)**2+ Ips)
       ,x=0..Om)));
  gma2[i,1,k]:=simplify(evalf(S2[1,i]*S2[1,i]*      # Cumulant-
generating function for -states
       lambda*
       Int(8*x**3*sqrt(Om**2-x**2)*
       (On**2-x**2)**2/
       (Pi*On*Om**6)*
    (exp(I*(-del-x)*times[k])-1-I*times[k]*(-del-x))/
       ((-del-x)**2+ Ips)
       ,x=0..Om)));
```

```
 end do:
end do:

# Main loop
for i from 1 to 3 do
 for j from 2 to nrstates do
  for k from 1 to N do
   del:= Eu[j] - El[j+i-2];                          # Energy
difference between vibronic states
   gma[i,j,k]:=simplify(evalf(S[j,i]*S[j,i]*         # Cumulant-
generating function for +states
       lambda*
       Int(8*x**3*sqrt(Om**2-x**2)*
       (On**2-x**2)**2/
       (Pi*On*Om**6)*
    (exp(I*(del-x)*times[k])-1-I*times[k]*(del-x))/
       ((del-x)**2+ Ips)
       ,x=0..Om)));
   gma2[i,j,k]:=simplify(evalf(S2[j,i]*S2[j,i]*   # Cumulant-
generating function for -states
       lambda*
       Int(8*x**3*sqrt(Om**2-x**2)*
       (On**2-x**2)**2/
       (Pi*On*Om**6)*
    (exp(I*(-del-x)*times[k])-1-I*times[k]*(-del-x))/
       ((-del-x)**2+ Ips)
       ,x=0..Om)));
  end do:
 end do:
end do:

for j from 1 to nrstates do
 for k from 1 to N do
  G[j,k] := evalf ( add ( gma[i,j,k], i=1..3));      # Summation
of cumulant-generating function over all vibronic levels
  G2[j,k]:= evalf ( add ( gma2[i,j,k], i=1..3));
 end do:
end do:

# Calculation of the Fourier transform of the spectra
for k from 1 to N do
 zw1[k]:=evalf((k-1)*Pi/T-(N-1)*Pi/(2*T)):          # Points in
the frequency domain where the spectrum is calculated
# Function of the spectrum in the time domain for the upper
potential
 rsu0[k] := evalf(add(Cu[j]*Cu[j]*exp(I*Eu[j]*times[k])*exp(
G[j,k] - g0*abs(times[k]))*(-1)**k, j=1..nrstates  )):
 rsu1[k] := evalf(add(cl[2,j]*cu[1,j]*exp(I*Eu[j]*times[k])*exp(
G[j,k] - g0*abs(times[k]))*(-1)**k, j=1..nrstates  )):
```

```
 rsu2[k] := evalf(add(cu[3,j]*cu[1,j]*exp(I*Eu[j]*times[k])*exp(
G[j,k] - g0*abs(times[k]))*(-1)**k, j=1..nrstates)):
# Function of the spectrum in the time domain for the lower
potential
 rsl0[k] := evalf(add(Cl[j]*Cl[j]*exp(I*El[j]*times[k])*exp(
G2[j,k] - g0*abs(times[k]))*(-1)**k, j=1..nrstates  )):
 rsl1[k] := evalf(add(cu[2,j]*cl[1,j]*exp(I*El[j]*times[k])*exp(
G2[j,k] - g0*abs(times[k]))*(-1)**k, j=1..nrstates  )):
 rsl2[k] := evalf(add(cl[3,j]*cl[1,j]*exp(I*El[j]*times[k])*exp(
G2[j,k] - g0*abs(times[k]))*(-1)**k, j=1..nrstates)):
end do:

for j from 1 to nrstates do
 for k from 1 to N do
# Function of the spectrum in the time domain for the upper
potential for each vibronic line
  rsu[j,k] := evalf(Cu[j]*Cu[j]*exp(I*Eu[j]*times[k])*exp (
G[j,k] - g0*abs(times[k]))*(-1)**k):
# Function of the spectrum in the time domain for the lower
potential for each vibronic line
  rsl[j,k] := evalf(Cl[j]*Cl[j]*exp(I*El[j]*times[k])*exp (
G2[j,k] - g0*abs(times[k]))*(-1)**k):
 end do:
end do:

RSU0fr:= FourierTransform(rsu0,N):                    # Fourier
transform from time to frequency domain
RSU1fr:= FourierTransform(rsu1,N):
RSU2fr:= FourierTransform(rsu2,N):
RSL0fr:= FourierTransform(rsl0,N):
RSL1fr:= FourierTransform(rsl1,N):
RSL2fr:= FourierTransform(rsl2,N):
RSUfr:= FourierTransform(rsu,2):
RSLfr:= FourierTransform(rsl,2):

for k from 1 by 1 to N do                             # Separating
the spectrum from the Fourier transform
 RSU0[k]:=Re(RSU0fr[k])*(-1)**k:
 RSL0[k]:=Re(RSL0fr[k])*(-1)**k:
 RSU1[k]:=Re(RSU1fr[k]*conjugate(RSU1fr[k])):
 RSU2[k]:=Re(RSU2fr[k]*conjugate(RSU2fr[k])):
 RSL1[k]:=Re(RSL1fr[k]*conjugate(RSL1fr[k])):
 RSL2[k]:=Re(RSL2fr[k]*conjugate(RSL2fr[k])):
 for j from 1 to nrstates do
  RSU[j,k]:=Re(RSUfr[j,k])*(-1)**k:
  RSL[j,k]:=Re(RSLfr[j,k])*(-1)**k:
 end do:
end do:
```

B.2 Code for calculating the relaxation

```
> # MAPLE packages used by the program
with(LinearAlgebra):
with(DiscreteTransforms):
with(orthopoly):

# Parameters of the calculation
Split:= 3;                          # Half splitting
between quasidegenerate states
Vibr:=10;                           # Vibrational coupling
strength
n := 100;                           # Number of vibrational
levels to be calculated
N:= 10;                             # Maximum level number
to be taken into account
g0:=0.02;                           # Parameter that
determines the line lifetime from other effects
lambda := 0.03;                     # Constant that
determines the strength of the phonon coupling
Om := 1.3;                          # Maximum frequency of
phonons
On := 1;                            # Frequency of the main
vibrational mode
nrtimesteps:=100;                   # Number of points in
time domain where relaxation is to be calculated
T:= 100;                            # Lenght of the time
domain of the relaxation process
distance:= 12;                      # Number of points in
configurational coordinate domain where relaxation is to be
calculated
nrdissteps:= 200;                   # Lenght of the
configurational coordinate domain of the relaxation process

# Variables of the claculation
A := Matrix(1..n,1..n, shape=symmetric ):   # Matrix of the
vibronic coupling
B := Matrix(1..n,1..n, shape=symmetric ):
#gma := Matrix(1..N,1..N);

# Solving of the vibronic Hamiltonian
for i from 1 to n do                # Initial setup of the
elements on the main diagonal
 A[i,i]:=(i-1) + ((-1)**(i-1))*Split :
```

```
 B[i,i]:=(i-1) + ((-1)**(i))*Split :
end do:

for s from 1 by 1 to (n-1) do       # Initial setup of the
off-diagonal elements
 A[s+1,s]:= evalf(sqrt (s*Vibr)) :
 B[s+1,s]:= evalf(sqrt (s*Vibr)) :
end do:

(Es,cs) := Eigenvectors(A):         # Solving the
eigenvalue problem
(Et,ct) := Eigenvectors(B):

for i from 1 by 2 to n-1 do         # Sorting the
eigenvalues and eigenvectors associated with the upper and
lower potential
 Eu[i] := Es[i]:
 Eu[i+1] := Et[i+1]:
 El[i]:= Et[i]:
 El[i+1]:= Es[i+1]:

 for j from 1 to n do
  cu[i,j]:= cs[i,j]:
  cu[i+1,j]:= ct[i+1,j]:
  cl[i,j]:= ct[i,j]:
  cl[i+1,j]:= cs[i+1,j]:
 end do:
end do:

# Calculation of the cumulant-generating function
for i from 1 to N do
 for j from 1 to N do   #
  del:= Eu[i] - El[j];
  gma[i,j]:=Re(evalf(lambda*(add(
  cu[2*k,j]*(sqrt(2*k-1)*cl[2*k-1,j]+
sqrt(2*k)*cl[2*k+1,j])+cl[2*k,j]*(sqrt(2*k-1)* cu[2*k-1,j]+
sqrt(2*k)* cu[2*k+1,j])
  ,k = 1..n/2-1 )**2)*8*del**3*sqrt(Om**2-del**2)*((On**2-
del**2)**2+0.1)/(Pi*On*Om**6))):
  gma2[i,j]:=Re(evalf(lambda*(add(
  cl[2*k,j]*(sqrt(2*k-1)*cu[2*k-1,j]+
sqrt(2*k)*cu[2*k+1,j])+cu[2*k,j]*(sqrt(2*k-1)* cl[2*k-1,j]+
sqrt(2*k)* cl[2*k+1,j])
```

```
  ,k = 1..n/2-1 )**2)*8*del**3*sqrt(Om**2-del**2)*((On**2-
del**2)**2+0.1)/(Pi*On*Om**6))):
 end do:
end do:

# Creation of the time-dependent functions used in
differential equations
for i to N do rhop[i] := (cat(xp, i))(t) end do:
for i to N do rhom[i] := (cat(xm, i))(t) end do:

# Creation of the differential equations to be solved
eq[1]:= diff(rhop[1],t) = -
(Heaviside(gma[1,1])*(g0+gma[1,1])*t*rhop[1]+Heaviside(-
gma2[1,1])*(-g0+gma[1,1])*t * rhom[1] + (-g0+gma2[1,2])*t *
rhom[2]):
eq[N+1]:= diff(rhom[1],t) = Heaviside(-gma2[1,1])*(-
g0+gma[1,1])*t*rhom[1] +
Heaviside(gma[1,1])*(g0+gma[1,1])*t * rhop[1] + (g0+
gma[2,1])*t * rhop[2]:

for i from 2 to N-1 do
 eq[i]:= diff(rhop[i],t) = -
((Heaviside(gma[i,i])*gma[i,i]+g0+gma[i,i-1] )*t*rhop[i] +
Heaviside(-gma2[i,i])*gma2[i,i]*t * rhom[i] + (-
g0+gma2[i,i+1])*t * rhom[i+1]) ;
 eq[N+i]:= diff(rhom[i],t) = (Heaviside(-
gma2[i,i])*gma2[i,i]-g0+gma2[i-1,i] )*t*rhom[i] +
Heaviside(gma[i,i])*gma[i,i]*t * rhop[i] +
(g0+gma[i+1,i])*t * rhop[i+1] ;
end do:

eq[N]:= diff(rhop[N],t) = -
((Heaviside(gma[N,N])*gma[N,N]+g0+gma[N,N-1]
)*t*rhop[N]+Heaviside(-gma2[N,N])*gma2[N,N]*t * rhom[N]):
eq[2*N]:= diff(rhom[N],t) = (Heaviside(-
gma2[N,N])*gma2[N,N]-g0+gma2[N-1,N]
)*t*rhom[N]+Heaviside(gma[N,N])*gma[N,N]*t * rhop[N]:

# Initial conditions
for i from 1 to N do
 IC[i]:= cat(xp,i)(0)= cu[1,i]**2 ;
 IC[N+i]:= cat(xm,i)(0)= cl[1,i]**2 ;
end do:
```

```
# Calculation of the time points used
for j from 0 to nrtimesteps do
 tt[j]:= evalf(j*T/nrtimesteps);
end do:

# Solving the diffrential equation numerically in specified
time points
dsol:= dsolve({seq(eq[j],j=1..2*N
),seq(IC[j],j=1..2*N)},numeric,[seq(rhop[j],j=1..N
),seq(rhom[j],j=1..N
)],output=Array([seq(tt[j],j=0..nrtimesteps)])):


# Calculation of the coordinate points used
for Q from 0 to nrdissteps do
 qq[Q] := evalf(Q*distance/nrdissteps):
end do:

# Calculation of the normalized wave functions
for k from 0 to n/2-1 do
 normalize:=0:
 for Q from 0 to nrdissteps do
  Wave[k+1,Q]:=
evalf(sqrt(1/(2**(2*k)*factorial(2*k)))*(On/Pi)**(0.25)*exp
(-sqrt(On)/2*qq[Q]**2)*H(2*k,sqrt(On)*qq[Q])):
  normalize:=normalize+Wave[k+1,Q]**2:
 end do:
 for Q from 0 to nrdissteps do
  Wave[k+1,Q]:= Wave[k+1,Q]/sqrt(normalize):
 end do:
end do:

# Calculation of the probability function
for t from 0 to nrtimesteps do
 for Q from 0 to nrdissteps do
  PP[Q,t]:= evalf(add(dsol[2,1][t+1,nu+1]*add ((
cu[2*k+1,nu]* Wave[k+1,Q],k=0..n/2-1))**2, nu=1..N ));
  PM[Q,t]:= evalf(add(dsol[2,1][t+1,nu+N+1]*add ((
cl[2*k+1,nu]* Wave[k+1,Q],k=0..n/2-1))**2, nu=1..N ));
 end do:
end do:
```

REFERENCES

[1] H. A. Jahn, E. Teller, *Proc. R. Soc. London A*, **161**, 220-235, (1937).
[2] R. Renner, *Z. Phys.*, **92**, 172, (1934).
[3] U.Öpik and M.H.Pryce, *Proc. R. Soc. London A*, **238**, 425-447, (1957).
[4] I. B. Bersuker, N.N. Gorinchoi, V. Z. Polinger, *Theor. Chim. Acta*, **66**, 161-172, (1984).
[5] P. Garcia-Fernandez, I. B. Bersuker, J. E. Boggs, *J. Phys. Chem. A*, **111**, 10409-10415, (2007).
[6] I. B. Bersuker, *Fundamental World of Quantum Chemistry*, Vol. 3, Eds. E.J. Brandas, E.S.Kryachko, Dordrecht, Kluwer, (2004).
[7] R. Englman, *The Jahn–Teller Effect in Molecules and Crystals*, Wiley, London, (1972).
[8] I. B. Bersuker, *The Jahn–Teller Effect,* Cambridge University Press, Cambridge, (2006).
[9] H. Köppel, D. R. Yarkony, H. Barentzen (Eds.), *The Jahn-Teller Effect: Fundamentals and Implicaions for Physics and Chemistry*, Springer, Berlin, (2009).
[10] K. Rebane, *Impurity Spectra of Solids: Elementary theory of vibrational structure*, Plenum Press, New York, (1970).
[11] R. L. Fulton, M. Gouterman, *J. Chem. Phys.*, **35**, 1059, (1961).
[12] M. C. M. O'Brien, *J. Phys. C: Solid State Phys.*, **5**, 2045, (1972).
[13] K. Pae, V. Hizhnyakov, *J. Chem. Phys*, **138**, 104103 (2013).
[14] I. B. Bersuker, V. Z. Polinger, *Vibronic interactions in Molecules and Crystals*, New York, Springer, (1989).
[15] V. Loorits, *Manifestations of the Fermi resonace in optical spectra of pseudo-Jahn–Teller effect*, Akademija Nauk ESSP, Otdelenije fiziko-matematicheskih nauk, Preprint F-11, (1979) (in Russian).
[16] R. P. Feynman, *Phys. Rev.*, **84**, 108, (1951).
[17] K. Pae, *Electronic transitions in symmetric systems of strong vibronic coupling.* Bachelor thesis, University of Tartu, (2008) (in Estonian).
[18] R. Kubo, Y. Toyozawa, *Prog. Theor. Phys.*, **13 (2)**, 160-182, (1955).
[19] M. Lax, *J. Chem. Phys.*, **20**, 1752, (1952).
[20] V. Hizhnyakov, I. Tehver, *J. Raman Spectroscopy*, **24**, 653, (1993).
[21] M. C. M. O'Brien, S. N. Evangelou, *Solid State Commun.*, **36**, 29, (1980).
[22] J. C. Slonczewski, *Phys. Rev.*, **131**, 1596, (1963).
[23] G. Lindblad, Commun. Math Phys., **48**, 119 ,(1976).
[24] H. D. Meyer, G. A. Worth, *Theor. Chem. Acc.*, **109**, 251, (2003).

PUBLICATIONS

CURRICULUM VITAE

Name: Taavi Vaikjärv
Date of birth: October 6, 1985, Tallinn, Estonia
Citizenship: Estonian
E-mail: taavi.vaikjärv@ut.ee

Education:

2009–2014	University of Tartu, PhD studies
2007–2009	University of Tartu, MSc (teacher of physics)
2004–2007	University of Tartu, BSc (physics)
2001–2004	Tallinn Secondary Science School
1992–2001	Tallinn German Secondary School of Kadriorg

Languages:
Estonian (mother-tongue), English, German

Professional employment:

2013–2014	University of Tartu, specialist
2011–2013	University of Tartu, curriculum manager
2009–2013	University of Tartu, engineer

Scientific and research activity:
Natural Sciences and Engineering – Physics and Technical Physics (condensed matter)

Other Activities:

2009–2013	Board of the Faculty of Science and Technology, University of Tartu, member

Publications:

1. V. Hizhnyakov, K. Pae, T. Vaikjärv Vibronic Transitions to a State with Jahn-Teller Effect: Contribution of Phonons, in Vibronic Interactions and the Jahn-Teller Effect: Theory and Applications, M.Atanasov et al. (Eds.), (2012), 179–191, Springer.
2. V. Hizhnyakov, V. Boltrushko, K. Pae, T. Vaikjarv, Zero-phonon lines: Novel manifestations of vibronic interactions in impurity centres of solids. Optika i Spektroskopiya, 111(3), (2011), 398–406.
3. I. Tehver, G. Benedek, V. Boltrushko, V. Hizhnyakov, T. Vaikjärv, Raman Scattering for Weakened Bonds in the Intermediate States of Impurity Centres. in M.Atanasov et al. (Eds.). Vibronic Interactions and the Jahn-Teller Effect: Theory and Applications, (2012), 163–177, Springer
4. V. Hizhnyakov, K. Pae, T. Vaikjärv. Optical Jahn-Teller effect in the case of local modes and phonons. Chemical Physics Letters, 525–526, (2012), 64–68.

5. T. Vaikjärv, V. Hizhnyakov, Time-dependent pseudo Jahn-Teller effect: Phonon-mediated long-time nonadiabatic relaxation. Journal of Chemical Physics, 140(6), (2014), 064105

ELULOOKIRJELDUS

Nimi: Taavi Vaikjärv
Sünniaeg: 06. oktoober, 1985, Tallinn, Eesti
Kodakondsus: Eesti
E-mail: taavi.vaikjarv@ut.ee

Haridustee:

2009–2014	Tartu Ülikool, doktorant
2007–2009	Tartu Ülikool, MSc (füüsikaõpetaja)
2004–2007	Tartu Ülikool, BSc (füüsika)
2001–2004	Tallinna Reaalkool
1992–2001	Tallinna Kadrioru Saksa Gümnaasium

Keeleoskus:
Eesti (emakeel), inglise, saksa

Teenistuskäik:

2013–2014	Tartu Ülikool, spetsialist
2011–2013	Tartu Ülikool, programmijuht
2009–2013	Tartu Ülikool, insener

Teadus- ja arendustegevus:
Loodusteadused ja tehnika – füüsika (kondentsaine teooria)

Muu tegevus:

2009–2013	Tartu Ülikooli loodus- ja tehnoloogiateaduskonna nõukogu liige

Publikatsioonid:

1. V. Hizhnyakov, K. Pae, T. Vaikjärv Vibronic Transitions to a State with Jahn-Teller Effect: Contribution of Phonons, in Vibronic Interactions and the Jahn-Teller Effect: Theory and Applications, M.Atanasov et al. (Eds.), (2012), 179–191, Springer.
2. V. Hizhnyakov, V. Boltrushko, K. Pae, T. Vaikjarv, Zero-phonon lines: Novel manifestations of vibronic interactions in impurity centres of solids. Optika i Spektroskopiya, 111(3), (2011), 398–406.
3. I. Tehver, G. Benedek, V. Boltrushko, V. Hizhnyakov, T. Vaikjärv, Raman Scattering for Weakened Bonds in the Intermediate States of Impurity Centres. in M.Atanasov et al. (Eds.). Vibronic Interactions and the Jahn-Teller Effect: Theory and Applications, (2012), 163–177, Springer
4. V. Hizhnyakov, K. Pae, T. Vaikjärv. Optical Jahn-Teller effect in the case of local modes and phonons. Chemical Physics Letters, 525–526, (2012), 64–68.

5. T. Vaikjärv, V. Hizhnyakov, Time-dependent pseudo Jahn-Teller effect: Phonon-mediated long-time nonadiabatic relaxation. Journal of Chemical Physics, 140(6), (2014), 064105

DISSERTATIONES PHYSICAE UNIVERSITATIS TARTUENSIS

1. **Andrus Ausmees.** XUV-induced electron emission and electron-phonon interaction in alkali halides. Tartu, 1991.
2. **Heiki Sõnajalg.** Shaping and recalling of light pulses by optical elements based on spectral hole burning. Tartu, 1991.
3. **Sergei Savihhin.** Ultrafast dynamics of F-centers and bound excitons from picosecond spectroscopy data. Tartu, 1991.
4. **Ergo Nõmmiste.** Leelishalogeniidide röntgenelektronemissioon kiiritamisel footonitega energiaga 70–140 eV. Tartu, 1991.
5. **Margus Rätsep.** Spectral gratings and their relaxation in some low-temperature impurity-doped glasses and crystals. Tartu, 1991.
6. **Tõnu Pullerits.** Primary energy transfer in photosynthesis. Model calculations. Tartu, 1991.
7. **Olev Saks.** Attoampri diapasoonis voolude mõõtmise füüsikalised alused. Tartu, 1991.
8. **Andres Virro.** AlGaAsSb/GaSb heterostructure injection lasers. Tartu, 1991.
9. **Hans Korge.** Investigation of negative point discharge in pure nitrogen at atmospheric pressure. Tartu, 1992.
10. **Jüri Maksimov.** Nonlinear generation of laser VUV radiation for high-resolution spectroscopy. Tartu, 1992.
11. **Mark Aizengendler.** Photostimulated transformation of aggregate defects and spectral hole burning in a neutron-irradiated sapphire. Tartu, 1992.
12. **Hele Siimon.** Atomic layer molecular beam epitaxy of A^2B^6 compounds described on the basis of kinetic equations model. Tartu, 1992.
13. **Tõnu Reinot.** The kinetics of polariton luminescence, energy transfer and relaxation in anthracene. Tartu, 1992.
14. **Toomas Rõõm.** Paramagnetic H^{2-} and F^+ centers in CaO crystals: spectra, relaxation and recombination luminescence. Tallinn, 1993.
15. **Erko Jalviste.** Laser spectroscopy of some jet-cooled organic molecules. Tartu, 1993.
16. **Alvo Aabloo.** Studies of crystalline celluloses using potential energy calculations. Tartu, 1994.
17. **Peeter Paris.** Initiation of corona pulses. Tartu, 1994.
18. **Павел Рубин.** Локальные дефектные состояния в CuO_2 плоскостях высокотемпературных сверхпроводников. Тарту, 1994.
19. **Olavi Ollikainen.** Applications of persistent spectral hole burning in ultrafast optical neural networks, time-resolved spectroscopy and holographic interferometry. Tartu, 1996.
20. **Ülo Mets.** Methodological aspects of fluorescence correlation spectroscopy. Tartu, 1996.
21. **Mikhail Danilkin.** Interaction of intrinsic and impurity defects in CaS:Eu luminophors. Tartu, 1997.

22. **Ирина Кудрявцева.** Создание и стабилизация дефектов в кристаллах KBr, KCl, RbCl при облучении ВУФ-радиацией. Тарту, 1997.
23. **Andres Osvet.** Photochromic properties of radiation-induced defects in diamond. Tartu, 1998.
24. **Jüri Örd.** Classical and quantum aspects of geodesic multiplication. Tartu, 1998.
25. **Priit Sarv.** High resolution solid-state NMR studies of zeolites. Tartu, 1998.
26. **Сергей Долгов.** Электронные возбуждения и дефектообразование в некоторых оксидах металлов. Тарту, 1998.
27. **Kaupo Kukli.** Atomic layer deposition of artificially structured dielectric materials. Tartu, 1999.
28. **Ivo Heinmaa.** Nuclear resonance studies of local structure in $RBa_2Cu_3O_{6+x}$ compounds. Tartu, 1999.
29. **Aleksander Shelkan.** Hole states in CuO_2 planes of high temperature superconducting materials. Tartu, 1999.
30. **Dmitri Nevedrov.** Nonlinear effects in quantum lattices. Tartu, 1999.
31. **Rein Ruus.** Collapse of 3d (4f) orbitals in 2p (3d) excited configurations and its effect on the x-ray and electron spectra. Tartu, 1999.
32. **Valter Zazubovich.** Local relaxation in incommensurate and glassy solids studied by Spectral Hole Burning. Tartu, 1999.
33. **Indrek Reimand.** Picosecond dynamics of optical excitations in GaAs and other excitonic systems. Tartu, 2000.
34. **Vladimir Babin.** Spectroscopy of exciton states in some halide macro- and nanocrystals. Tartu, 2001.
35. **Toomas Plank.** Positive corona at combined DC and AC voltage. Tartu, 2001.
36. **Kristjan Leiger.** Pressure-induced effects in inhomogeneous spectra of doped solids. Tartu, 2002.
37. **Helle Kaasik.** Nonperturbative theory of multiphonon vibrational relaxation and nonradiative transitions. Tartu, 2002.
38. **Tõnu Laas.** Propagation of waves in curved spacetimes. Tartu, 2002.
39. **Rünno Lõhmus.** Application of novel hybrid methods in SPM studies of nanostructural materials. Tartu, 2002.
40. **Kaido Reivelt.** Optical implementation of propagation-invariant pulsed free-space wave fields. Tartu, 2003.
41. **Heiki Kasemägi.** The effect of nanoparticle additives on lithium-ion mobility in a polymer electrolyte. Tartu, 2003.
42. **Villu Repän.** Low current mode of negative corona. Tartu, 2004.
43. **Алексей Котлов.** Оксианионные диэлектрические кристаллы: зонная структура и электронные возбуждения. Tartu, 2004.
44. **Jaak Talts.** Continuous non-invasive blood pressure measurement: comparative and methodological studies of the differential servo-oscillometric method. Tartu, 2004.
45. **Margus Saal.** Studies of pre-big bang and braneworld cosmology. Tartu, 2004.

46. **Eduard Gerškevitš.** Dose to bone marrow and leukaemia risk in external beam radiotherapy of prostate cancer. Tartu, 2005.
47. **Sergey Shchemelyov.** Sum-frequency generation and multiphoton ionization in xenon under excitation by conical laser beams. Tartu, 2006.
48. **Valter Kiisk.** Optical investigation of metal-oxide thin films. Tartu, 2006.
49. **Jaan Aarik.** Atomic layer deposition of titanium, zirconium and hafnium dioxides: growth mechanisms and properties of thin films. Tartu, 2007.
50. **Astrid Rekker.** Colored-noise-controlled anomalous transport and phase transitions in complex systems. Tartu, 2007.
51. **Andres Punning.** Electromechanical characterization of ionic polymer-metal composite sensing actuators. Tartu, 2007.
52. **Indrek Jõgi.** Conduction mechanisms in thin atomic layer deposited films containing TiO_2. Tartu, 2007.
53. **Aleksei Krasnikov.** Luminescence and defects creation processes in lead tungstate crystals. Tartu, 2007.
54. **Küllike Rägo.** Superconducting properties of MgB_2 in a scenario with intra- and interband pairing channels. Tartu, 2008.
55. **Els Heinsalu.** Normal and anomalously slow diffusion under external fields. Tartu, 2008.
56. **Kuno Kooser.** Soft x-ray induced radiative and nonradiative core-hole decay processes in thin films and solids. Tartu, 2008.
57. **Vadim Boltrushko.** Theory of vibronic transitions with strong nonlinear vibronic interaction in solids. Tartu, 2008.
58. **Andi Hektor.** Neutrino Physics beyond the Standard Model. Tartu, 2008.
59. **Raavo Josepson.** Photoinduced field-assisted electron emission into gases. Tartu, 2008.
60. **Martti Pärs.** Study of spontaneous and photoinduced processes in molecular solids using high-resolution optical spectroscopy. Tartu, 2008.
61. **Kristjan Kannike.** Implications of neutrino masses. Tartu, 2008.
62. **Vigen Issahhanjan.** Hole and interstitial centres in radiation-resistant MgO single crystals. Tartu, 2008.
63. **Veera Krasnenko.** Computational modeling of fluorescent proteins. Tartu, 2008.
64. **Mait Müntel.** Detection of doubly charged higgs boson in the CMS detector. Tartu, 2008.
65. **Kalle Kepler.** Optimisation of patient doses and image quality in diagnostic radiology. Tartu, 2009.
66. **Jüri Raud.** Study of negative glow and positive column regions of capillary HF discharge. Tartu, 2009.
67. **Sven Lange.** Spectroscopic and phase-stabilisation properties of pure and rare-earth ions activated ZrO_2 and HfO_2. Tartu, 2010.
68. **Aarne Kasikov.** Optical characterization of inhomogeneous thin films. Tartu, 2010.

69. **Heli Valtna-Lukner.** Superluminally propagating localized optical pulses. Tartu, 2010.
70. **Artjom Vargunin.** Stochastic and deterministic features of ordering in the systems with a phase transition. Tartu, 2010.
71. **Hannes Liivat.** Probing new physics in e+e− annihilations into heavy particles via spin orientation effects. Tartu, 2010.
72. **Tanel Mullari.** On the second order relativistic deviation equation and its applications. Tartu, 2010.
73. **Aleksandr Lissovski.** Pulsed high-pressure discharge in argon: spectroscopic diagnostics, modeling and development. Tartu, 2010.
74. **Aile Tamm.** Atomic layer deposition of high-permittivity insulators from cyclopentadienyl-based precursors. Tartu, 2010.
75. **Janek Uin.** Electrical separation for generating standard aerosols in a wide particle size range. Tartu, 2011.
76. **Svetlana Ganina.** Hajusandmetega ülesanded kui üks võimalus füüsikaõppe efektiivsuse tõstmiseks. Tartu, 2011
77. **Joel Kuusk.** Measurement of top-of-canopy spectral reflectance of forests for developing vegetation radiative transfer models. Tartu, 2011.
78. **Raul Rammula**. Atomic layer deposition of HfO_2 – nucleation, growth and structure development of thin films. Tartu, 2011.
79. **Сергей Наконечный.** Исследование электронно-дырочных и интерстициал-вакансионных процессов в монокристаллах MgO и LiF методами термоактивационной спектроскопии. Тарту, 2011.
80. **Niina Voropajeva.** Elementary excitations near the boundary of a strongly correlated crystal. Tartu, 2011.
81. **Martin Timusk.** Development and characterization of hybrid electro-optical materials. Tartu, 2012, 106 p.
82. **Merle Lust.** Assessment of dose components to Estonian population. Tartu, 2012, 84 p.
83. **Karl Kruusamäe.** Deformation-dependent electrode impedance of ionic electromechanically active polymers. Tartu, 2012, 128 p.
84. **Liis Rebane.** Measurement of the $W \to \tau\nu$ cross section and a search for a doubly charged Higgs boson decaying to τ-leptons with the CMS detector. Tartu, 2012, 156 p.
85. **Jevgeni Šablonin.** Processes of structural defect creation in pure and doped MgO and NaCl single crystals under condition of low or super high density of electronic excitations. Tartu, 2013, 145 p.
86. **Riho Vendt**. Combined method for establishment and dissemination of the international temperature scale. Tartu, 2013, 108 p.
87. **Peeter Piksarv.** Spatiotemporal characterization of diffractive and non-diffractive light pulses. Tartu, 2013, 156 p.
88. **Anna Šugai.** Creation of structural defects under superhigh-dense irradiation of wide-gap metal oxides. Tartu, 2013, 108 p.

89. **Ivar Kuusik.** Soft X-ray spectroscopy of insulators. Tartu, 2013, 113 p.
90. **Viktor Vabson**. Measurement uncertainty in Estonian Standard Laboratory for Mass. Tartu, 2013, 134 p.
91. **Kaupo Voormansik.** X-band synthetic aperture radar applications for environmental monitoring. Tartu, 2014, 117 p.
92. **Deivid Pugal.** hp-FEM model of IPMC deformation. Tartu, 2014, 143 p.
93. **Siim Pikker.** Modification in the emission and spectral shape of photostable fluorophores by nanometallic structures. Tartu, 2014, 98 p.
94. **Mihkel Pajusalu**. Localized Photosynthetic Excitons. Tartu, 2014, 183 p.